AN INVESTIGATION ON TEXTURE-PROPERTY CORRELATION IN COLD-ROLLED NON-ORIENTED SILICON STEELS

A Thesis Submitted in Partial Fulfillment of the Requirements for the Degree of

Bachelor of Technology

in

METALLURGICAL AND MATERIALS ENGINEERING

by

DIBYARANJAN PRUSTY (108MM007)

HITAINDRA KUMAR PRADHAN (108MM041)

DEPARTMENT OF METALLURGICAL AND MATERIALS ENGINEERING

NATIONAL INSTITUTE OF TECHNOLOGY

ROURKELA

May, 2012

AN INVESTIGATION ON TEXTURE-PROPERTY CORRELATION IN COLD-ROLLED NON-ORIENTED SILICON STEELS

A Thesis Submitted in Partial Fulfillment of the Requirements for the Degree of

Bachelor of Technology

in

METALLURGICAL AND MATERIALS ENGINEERING

by

DIBYARANJAN PRUSTY (108MM007)
HITAINDRA KUMAR PRADHAN (108MM041)

Under the Guidance of

PROF. SANTOSH KUMAR SAHOO

DEPARTMENT OF METALLURGICAL AND MATERIALS ENGINEERING
NATIONAL INSTITUTE OF TECHNOLOGY
ROURKELA
2012

National Institute of Technology

Rourkela

CERTIFICATE

This is to certify that the thesis entitled, " **An Investigation on Texture-Property Correlation in Cold Rolled Non-Oriented Silicon Steels"** submitted by **Dibyaranjan Prusty (108MM007)**, **Hitaindra Kumar Pradhan** (**108MM041**) in partial fulfillment of the requirements for the award of **Bachelor of Technology Degree** in **Metallurgical and Materials Engineering** at National Institute of Technology, Rourkela is an authentic work carried out by them under my supervision and guidance.

To the best of my knowledge, the matter embodied in the thesis has not been submitted to any other University/Institute for the award of any Degree or Diploma.

Prof. Santosh Kumar Sahoo
Dept. of Metallurgical and Materials Engineering
National Institute of Technology
Rourkela-769008

Date:

Acknowledgement

We take this opportunity to express our deep regards and sincere gratitude to our guide **Prof. Santosh Kumar Sahoo** for his constant guidance and concern throughout the project. He will always remain be a constant source of inspiration for us. We also express our sincere gratitude to, **Dr. B.C.Ray**, HOD, Metallurgical and Materials Engineering for providing valuable departmental facilities. We are very thankful to **Prof. Indradev Samajdar** of IIT Bombay, **Prof.B.B.Nayak** of Ceramic department NIT Rourkela, **Prof. S.karmakar** of Electrical department of NIT Rourkela and **Prof. D.K. Pradhan** of Physics department of NIT Rourkela for their constant support in conducting experiments. We extend our thanks to all the professors who have guided, suggested and helped us during the project. We are also thankful to technical assistants of Department of Metallurgical and Materials Engineering, NIT Rourkela, for their constant practical assistance and help whenever required. We would also like to thank all the staff members of **Metallurgical and Materials Engineering department** and everyone who in some way or the other has provided us valuable guidance, suggestion and help for this project.

Place: NIT Rourkela
Date:

Dibyaranjan Prusty (108MM007)
Hitaindra Kumar Pradhan (108MM041)

Abstract

Soft magnetic materials like cold rolled non-oriented (CRNO) steels are used in electrical appliances like motors, generators small transformer cores due to its superior magnetic permeability and low watt loss and less magnetic anisotropy signifying uniform magnetic properties in all directions. The application of CRNO steels demands uniform property in all angular directions. Keeping this in mind the objective of the present study is to find out the textural and property change in all angular directions of CRNO steel sheets and correlate texture-property. CRNO steel sheets of different silicon percentages (1.4%, 1.52%, 1.88%, and 2%) were observed in the present study. Four different sets of samples were made from the CRNO sheets: (1) samples along rolling direction, (2) samples at 30° to the rolling direction, (3) samples at 60° to the rolling direction and (4) samples at 90° to the rolling direction. Then the textural, electrical and magnetic properties were investigated using standard techniques. X-ray diffraction (XRD) and electron backscattered diffraction (EBSD) were used for bulk- and micro-texture measurements respectively. While four-probe method was used for electrical resistivity and pulse field hysteresis loop tracer was used for magnetic property measurements. The results showed different texture and magnetic properties in all the CRNO samples.

Keywords: CRNO steel, Silicon Steel, Electrical Steel, Texture, Magnetic Permeability, Watt Loss.

Content

List of figures

List of tables

CHAPTER -I

1.0 Introduction

Although, grain oriented silicon steels have attracted more academic interests [1], grain non-oriented silicon steels [2,3] (generically termed as CRNO or cold rolled non-grain oriented steel) are the highest tonnage of electrical steels being produced today. Major applications of CRNO steels are core material for electrical motor, rectifiers, generators, small size core transformers etc. They possess low core loss and high permeability for such applications [4]. Two important metallurgical factors that are responsible for the above said properties are grain size and texture [5]. As grain size increases, hysteresis loss decreases due to increase in domain width and eddy current loss increases [6]. So, there is an optimum grain size which determines the sum of hysteresis loss and eddy current loss to a minimum value. For example, the optimum grain sizes are100 micron and 150 micron for 1.85% and 3.2% Si steel respectively. The existence of an optimum grain size can be explained from domain theory, which can be demonstrated as, below the optimum grain size hysteresis loss due to domain wall interactions is predominant, while above the optimum grain size losses are linked to domain wall movement [7]. Material with a texture favorable for magnetic properties shows lower core loss than those with an unfavorable texture, although they have same grain size [8]. Unlike CRGO (cold rolled grain oriented) steels, a specific orientation cannot be considered in CRNO steels which are used in cores for rotating machines and in these machines the angle between directions of the applied electric field and rolling direction vary continuously. Texture components like (001)<*uvw*> and (111)<*uvw*> are considered respectively as good and bad texture components. (111)<uvw> is the worst texture for magnetic properties [9]. For a CRNO steel to stand in manufacture of components where texture, magnetic and electric properties are uniform in all direction unlike GOSS texture (110) <001> which dominates in CRGO steel. So, it's very important to link between metallurgical factors and magnetic properties while producing certain equipment [10]. In the present study the electrical and magnetic properties of ~1.5 (wt.%) and ~2.0 (wt.%) CRNO sheets were investigated with respect to all angular direction. In this way it has been attempted to link the texture and electrical/magnetic properties of the CRNO silicon steels.

1.1 Objectives

The various objectives which are to be achieved in the projects are:

- Study the variation in texture of CRNO steel sheets with respect to composition as well as angular direction.
- Determination of electrical properties such as resistivity and magnetic properties like core loss and permeability of all the CRNO steel samples.
- Correlation between texture, magnetic and electrical properties of CRNO steel samples.

1.2 Framework of the Thesis

The thesis is divided into five chapters. Chapter I mainly concerns about the introduction of the project work. Chapter II gives theoretical overview of CRNO steel, methods of representing texture, development of texture in CRNO steels and dependence of grain size on magnetic properties of silicon steels. Chapter III represents the details of CRNO steel and sample preparation followed by characterization techniques used in the present investigation. Chapter IV basically tells the results that are obtained by texture measurements, electrical and magnetic property measurements and discussion of the experimental results obtained. Chapter V summarizes the results obtained from the present study and hints the scopes for further works.

CHAPTER II

2.0 Literature Review

2.1 Silicon steel

Silicon steel, also known as electrical steel, is extensively used for electrical applications such as preferred core material for equipment like transformer cores, motors, and generators [11].The total amount of these steels is around 1% of the world production of steel. The properties required for these steels are a high permeability and high magnetic induction, low magnetic losses (watt losses), and low magnetostriction. The factors like high permeability and induction is effective in reducing the size and weight of the parts thus increases the efficiency; low magnetic losses reduce the generation of Joule heat and energy consumption thus helps in minimizing energy; and a low magnetostriction reduces the noise in transformers and high-capacity machines helps in producing less humming sound [12].

2.1.1 Effect of Si in Fe

In late 19^{th} century when discovery of silicon additions to increase the resistivity without affecting the saturation magnetization significantly, electrical steel was developed. The addition of silicon to iron has the following effects on its (magnetic) properties [13,14,15]:

(i) The electrical resistivity is increased, the eddy currents are diminished and the losses are lowered.

(ii) Magneto crystalline anisotropy decreases, causing an increase in the permeability.

(iii) The magnetostriction decreases, leading to smaller dimensional changes with magnetization and demagnetization process, and to a lower stress-sensitivity of the magnetic properties.

(iv) The saturation induction decreases.

(v) When the Si content is higher than 3%, the brittleness of the steel is increased and the cold deformability is significantly impaired.

Figure 2.1 shows the effect of silicon on magnetic properties of Fe-Si alloy.

There are generally two different types of silicon steel namely:

(i) Grain oriented silicon steel (GO)

(ii) Grain non-oriented silicon steel (GNO)

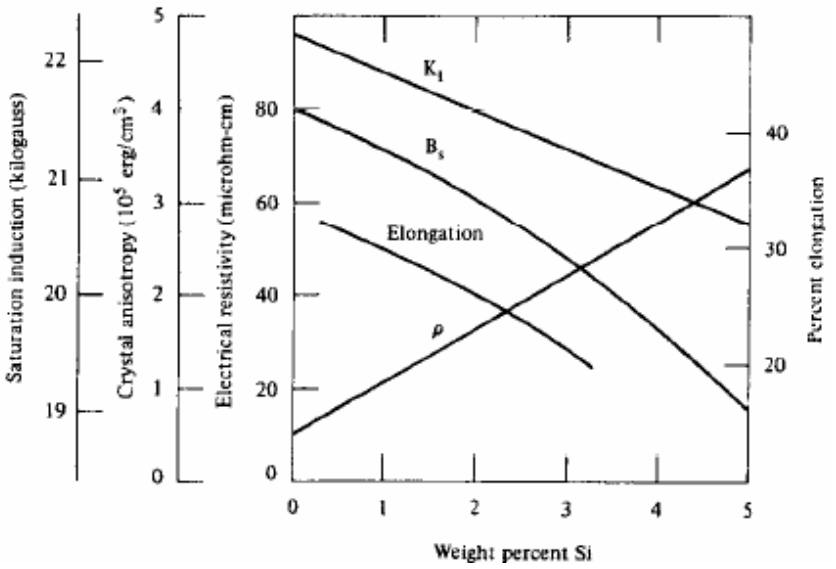

Figure 2.1. Effect of addition of Silicon on various properties like percentage of elongation,crystal anisotropy, saturation induction [16]

Silicon steels featuring high Goss texture (110)[001] are called grain oriented and are mainly used for core material for power and distribution transformers where the magnetic flux is unidirectional. The Goss texture has <100> direction, known as easy magnetization direction parallel to rolling direction. Although GO silicon steel has attracted more due to its properties , GNO steels are being the highest tonnage of electrical steels being produced today [17, 18]. Grain non-oriented silicon steel does not present a very high Goss texture and one of its main technological application advancement in rotating electrical machinery in which the magnetic field is in the plane of the sheet, but the angle between the electric and magnetic field and the rolling direction is variable (always changes) i.e. magnetic properties should be uniform all over the directions. Taking case of rotating machineries' like motors, there is no point in having the easiest direction of magnetization, i.e. <100>, parallel to the RD and an adequate texture would be {100}<uvw>, also known as <100> fiber texture [19], where most of the grains would have their {100} planes parallel to the plane of the sheet. The processing of GNO electrical steel comprises hot rolling which may be with annealing or without annealing, cold rolling in one or two steps with an intermediate annealing, final annealing and coating. The GNO steel may be termed as CRNO steel i.e. cold rolled non-oriented steel and GO steel as CRGO i.e. cold rolled grain oriented steel

2.2 Texture

As discussed earlier, orientation of grains/crystals is important in deciding the magnetic property of silicon steels. When the orientation of grains are statistically distributed at random, the material is said to be crystallographic isotropic and shows no preferred texture. However, if they are not randomly oriented, the material has a crystallographic texture. The term 'crystallographic' is used here only because the material can also show morphological texture [20]. Crystallographic texture can be represented either by pole figure (PF) or orientation distribution function (ODF).

2.2.1 Grain Orientation

It is very much important to know about grain orientation and its representation before going through PF and ODF. The orientation of a grain is always expressed relative to an external co-ordinate system. In flat products (plates, sheets), the external reference frame traditionally consists of the rolling direction (RD), the normal direction (ND) and the transverse direction (TD). Any crystal orientation can be expressed with the help of Miller indices and is written as: (*hkl*)[*uvw*]. This represents that the direction [*uvw*] is parallel with the RD and a plane (hkl) is parallel with the rolling plane. For example, the orientation of the crystal as in Figure 2.2(a) should be written as (001)[1-10]. When all the crystallographic equivalent orientations are considered, the Miller indices are expressed as {hkl}<uvw>. In axisymmetric products (wires, extruded bars), one set of Miller indices [*uvw*] is used to describe the crystal orientation, indicating that this crystallographic direction is parallel with the sample axis, e.g. [111] in Figure 2.2b. All rotations around [*uvw*] are crystallographic equivalent [21].

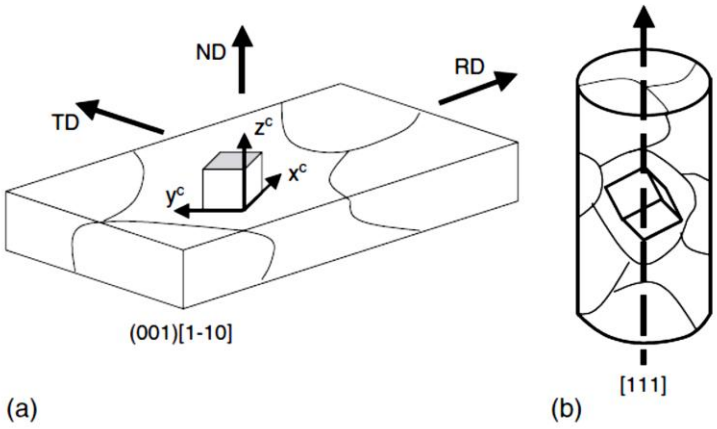

Figure 2.2. Examples of crystal orientations in sheet (a) and wire (b), expressed with Miller indices. The three cube axes are shown as x^c, y^c and z^c. [22]

2.2.2 Pole Figures

Pole figure is a projection, more often represented by a stereographic projection, by taking a particular orientation in relative to the sample, which shows the variation of density of poles or pole density with pole orientation for a selected set of crystal planes [23]. A schematic of (100) pole figure is shown in Figure 2.3. In figure 2.3, the Stereographic projection of (100) poles is represented in (a) and the projection of (100) poles of one grain on the equatorial plane is represented in (b). Figure 2.3c shows projection of the (100) poles of a polycrystal where the grains are randomly oriented. Figure 2.3d shows the projection of (100) poles of a textured polycrystal, and this is usually represented as contour maps – as shown in figure 2.3e.

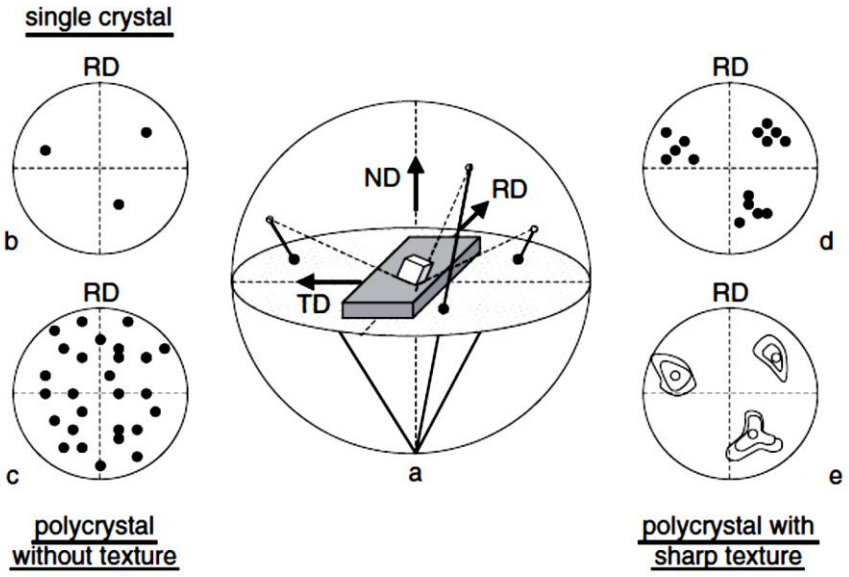

Figure 2.3. Schematic showing construction of a (100) pole figure [24].

2.2.4 Orientation Distribution Function (ODF)

Pole figure representation of texture has several limitations. During projection of an orientation, it is mandatory to miss certain orientations as a 3D space is represented in a 2D circle. It is necessary to analyze all orientations for complete understanding of texture of the material. With the help of ODF, it is possible to describe the complete texture information of a sample.If the orientation of a grain can be represented by a parameter '*g*'. An ODF is a mathematical series expansion, for which we will use the symbol 'f' that describes the volume fraction of grains in all intervals $g \pm dg$.

$$(dv/v)= f(g)dg$$

The integral of the ODF over all orientations should be equal to 1. ODF is used statistically to make all possible orientation of grain where no loss of data occurs and measurement of sample give accurate result. The ODF of a sample without any texture is a constant. If the sample possesses any texture, the ODF has maxima and minima [25].

2.2.4.1 Euler Angles

In order to give a graphical representation of an ODF, a suitable method must be adopted, which will define the orientation '*g'* of a grain. This is basically done with the help of 'Euler angles'. These Euler angles defined in order to describe the position of a particular orientation. Two different co-ordinate systems are defined and the method can be described as follows. The first is connected to the sample (sample axes system X_i) and the second to the crystal of a grain (crystal axes system X_i^c). Both systems are Cartesian and right handed (Figure 2.4). The sample system is related to the shape of the sample. Let us take an example of a rolled sheet, and the axis X_1 is taken in the rolling direction (RD) , X_2 in the transverse direction(TD) and X_3 in the normal direction (ND) of the sheet. Three rotations which are used to describe the orientation fully is shown (Figure 2.5). These three rotations bring both systems together. Literature shows, there are several conventions have been proposed to perform these rotations. The most widely used system is the system of Bunge [26].

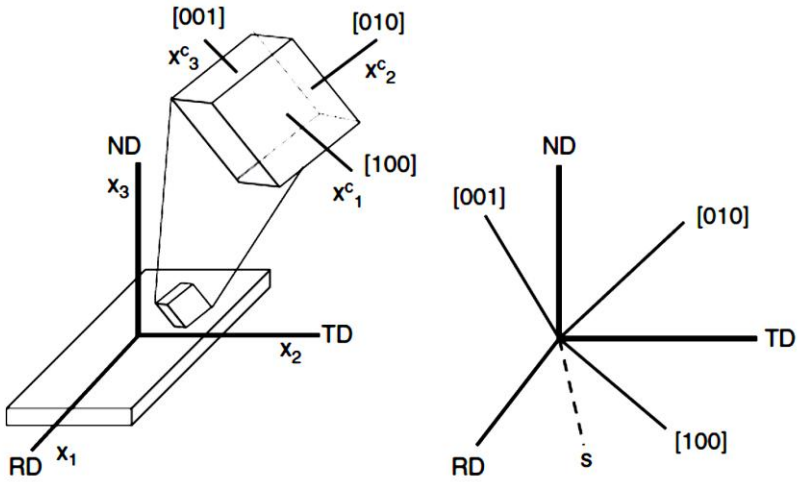

Figure 2.4. Orientation of the crystal axis system $\{X_i^c\}$ and the sample axis system {RD, TD, ND}; *s* is the intersection of the planes (RD–TD) and ([100]–[010]) [27].

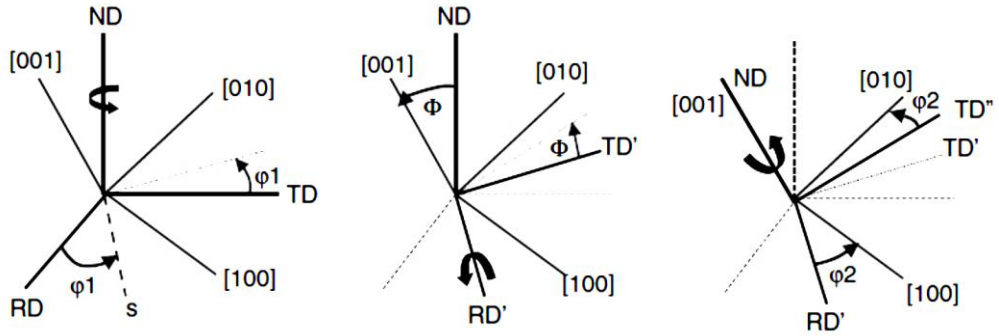

Figure 2.5. Definition of the Euler angles φ_1, Φ, and φ2 in the Bunge convention [28].

- At first a rotation φ_1 around ND is performed; which will bring RD in the position *s*, with *s* the intersection of the planes (RD–TD) and ([100]–[010]). The attainment of new positions of RD and TD are now RD' and TD'.
- Then, a rotation of Φ around RD'; this will bring ND together with [001]; TD' will now get the position TD'.
- Finally, a rotation of φ_2 around the ND axis (which is now equal to [001]); due to this rotation,vRD' falls on [100] and TD' comes together with [010]. The angles (φ_1, Φ, φ_2) are called 'Euler angles'.

2.2.4.2 Euler Space

To represent every orientation in space it is important to represent it with the help of three Euler angles or 2 Euler angles by keeping the other one constant. When three Euler angles are used it 3D representation of texture data and when 2 Euler angles are used by keeping other being constant it is called 2D representation of texture data which is normally used in real practice. When the three Euler angles are generally plotted in Cartesian coordinate system, we get the so-called 'Euler space'. This space is limited for φ_1 and φ_2 between 0^o and 360^o, and for between 0^o and 180^o (Figure 2.6). Each crystal orientation can be represented in this Euler space. In this representation, individual orientations will be found at several locations and at several euler angles of the Euler space [29].

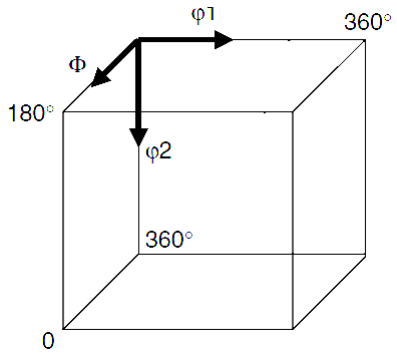

Figure 2.6. Graphical representation of crystallographic orientations with Euler angles [30].

2.3 Texture Developments in CRNO Silicon Steels

The magnetic properties like magnetization behavior and specific magnetic losses depends upon the texture of the steel. Crystallographic texture is very important in bcc iron because magnetization behavior is different along different direction. For example, <100> direction is the easy magnetization direction, <110> is the intermediate one and <111> is the hardest direction of magnetization [31]. So the planes having maximum <100> axis are preferred, planes having <110> direction are desirable and planes having <111> direction are avoided as far as possible [32]. The various texture components that are observed in a non-oriented electrical steels can be generally classified into 7 categories which are Goss {110}<100>, cube {100}<001>, rotated cube {110}<110>, theta {100}<uvw>, eta {hkl}<100>, gamma {111}<uvw> and alpha

{hkl}<110> [33]. Among these 7, cube texture is most desirable because {100} planes have greatest numbers of <100> axes. Texture with {110} planes have relatively larger number of <100> and <110> axes which are also desirable. On the other hand, the texture with {111} planes containing no <100> axes and the texture with {112} planes including <111> axes are undesirable for non-oriented steels. As a consequence, the ideal textures for non-oriented electrical steels is {100}<001>, Goss {110} <100>, theta {100} <uvw>, eta {hkl}<100>.

The final texture developed in any non-oriented steels is influenced by all the textures developed during every processing step i.e. hot rolling texture, hot band annealing texture, recrystallization texture and texture during grain growth which are described as follows:

In hot rolling the texture with low intensity of {110} <001> and {112} <111> are found [34]. Hot rolling also gives rotated cube {110}<110> orientation which is interesting for magnetic applications [35]. Hot-band annealing at a higher temperature is very effective to obtain both high magnetic induction and low core loss which are very essential, while it enhances the anisotropy of magnetic properties which is detrimental for a motor or generator manufacture [36]. These effects of hot-band annealing can be explained principally by the texture effect. The increase in planar anisotropy by hot-band annealing may be closely related to an increase in the {110} component and decreases in the {211} and {222} components. Recrystallization texture is one of the most important textures because the maximum texture property variation occurs between cold rolling and annealing when new strain free grains are induced from the strained lattice. The various texture components which are observed during recrystallization are namely Goss {110}<100>, cube {100}<001> and gamma fiber {111} <uvw> components [37]. The intensity of Goss component is strongest. The general rule which governs texture development during grain growth in electrical steels can be proposed as follows: for a texture component to be strengthened during grain growth the grains of specific orientations should have not only a size advantage over other orientations but also a higher frequency of high angle, high energy grain boundaries [38].

The texture of the final products is also greatly affected by the microstructure prior to cold rolling, the quantity of inclusions and the reduction of cold rolling. When a hot-rolled sheet is annealed to increase its grain size, the development of recrystallized grains with {111} planes, from the original grain boundary, is suppressed, whereas the development of recrystallized grains

with {100} planes is enhanced in cold-rolled and final-annealed products. Though, it requires more production cost the two-stage cold rolling method also being practiced to get better texture. For the benefit of the readers, the important orientations discussed above have been represented in Figure 2.7.

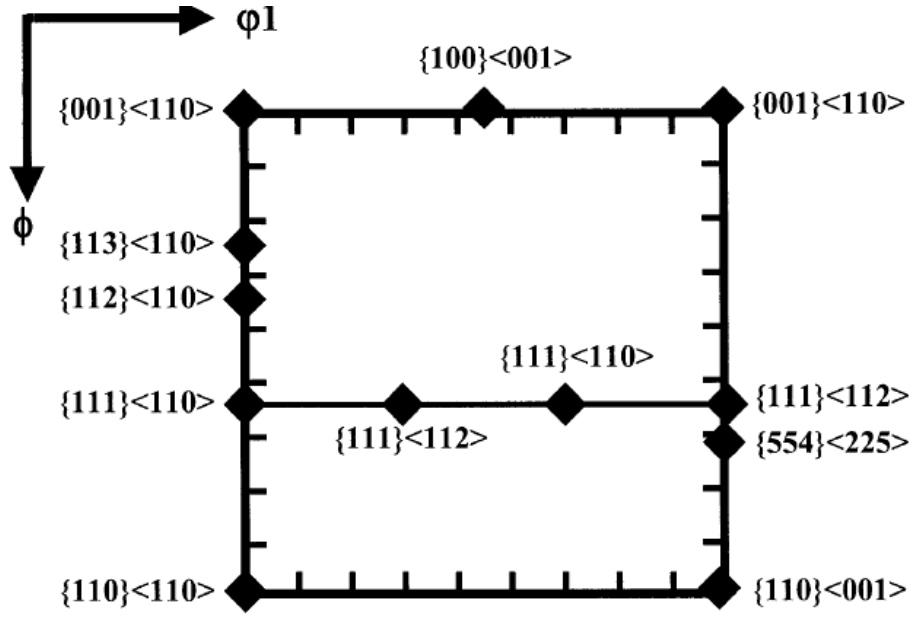

Figure 2.7. Schematic representation of the most important texture components in the φ_2=45° section of ODF [39].

2.4 Grain Size Dependence on Magnetic Properties of CRNO Silicon Steels

Grain sizes affect magnetic properties in both GO and GNO steels [40]. Figure 2.8 shows the effect of grain size on core loss in silicon steels of different silicon percentages [41]. An optimum grain size is desirable – see figure 2.8. This may be attributed due to magnetic domain wall interactions, as we know, below the optimum grain size hysteresis loss are mainly because of domain wall interactions, while above the optimum grain size losses are very much correlated to the domain wall movement concept [43].

This optimum grain size changes with composition and texture. To produce materials with low iron loss it is very much essential to promote grains to optimum size through a short-continuous

annealing [44]. So, it is very much necessary to avoid precipitates that are caused by C, S, N and O which hinder the growth of the grains. The effect of change in grain size was insignificant at smaller texture factor (TF), but noticeable at higher TF [45].Texture factor can be defined as the ratio of volume fraction of bad texture component to the volume fraction of bad texture component i.e. ({111}<uvw>/{100}<uvw>). With the decrease in texture factor the magnetic properties are improved and there is a decrease in magneto crystalline energy. In general, watt loss is decreased and permeability is increased at larger grain size and smaller TF.

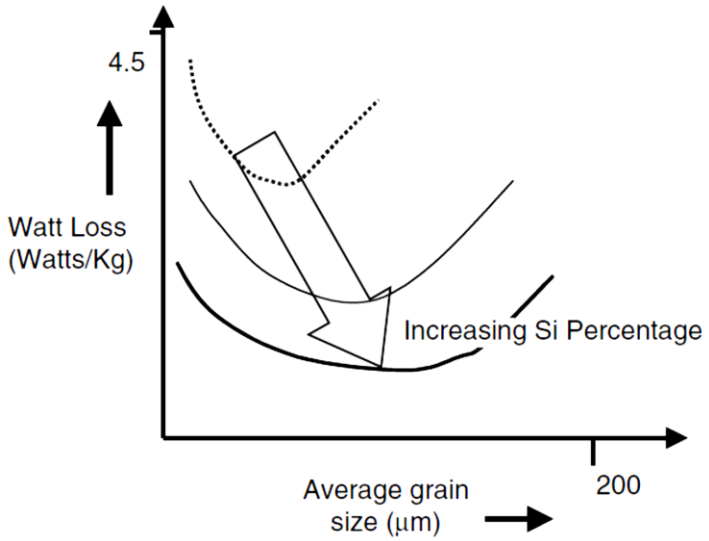

Figure 2.8. Effect of grain size on core loss in silicon steel [46].

CHAPTER III

3.0 Materials and Experimental Procedure

3.1 Materials

The materials studied in the present work were obtained from cold rolled steel sheets of 0.5 mm thickness with chemical compositions given in table 3.1. The CRNO steel was first hot rolled from continuously cast slabs of 210 mm thickness to 2.3 mm thick strips and subsequently cold rolled to 0.5 mm thick sheets. The full hard coils were batch annealed to 950˚C +/- 10˚ and finally given 2% deformation at the skin pass mill. Then DA (decarburization annealing) treatments were carried out in a controlled atmosphere (dry 75%N_2+25%H_2) muffle furnace at 840˚C.

Table 3.1. Different compositions (in wt. %) of CRNO steel samples. The balance amount is the wt. % Fe.

Steel Grade	C	Si	P	S	Mn	Al
A1	0.027	2.00	0.024	0.008	0.21	0.128
A2	0.027	1.88	0.015	0.009	0.20	0.170
A3	0.025	1.52	0.020	0.015	0.25	0.090
A4	0.024	1.40	0.020	0.025	0.19	0.075

From each grade of CRNO steel sheets, four samples were prepared – (1) in the rolling direction (A1-0, A2-0, A3-0 and A4-0); (2) 30˚ to the rolling direction (A1-30, A2-30, A3-30 and A4-30); (3) 60˚ to the rolling direction (A1-60, A2-60, A3-60 and A4-60) and (4) 90˚ to the rolling direction (A1-90, A2-90, A3-90 and A4-90) – see figure 3.2. The samples were metallographically polished and then electro-polished by using an electrolyte of 800ml glacial acetic acid and 200ml perchloric acid before textural characterization.

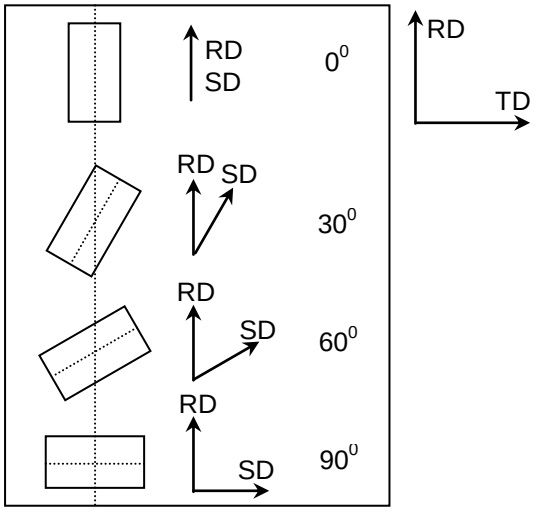

Figure 3.1. A schematic representing the samples prepared from CRNO steel sheets for the present investigation. RD, TD and SD represent the rolling direction, transverse direction and sample direction respectively.

3.2 Texture Characterization

3.2.1 Bulk/Macro Texture

A Panalytical MRD X-ray diffraction system is used for bulk texture characterization. This is available at IIT Bombay and is used for the present study. Four different pole figures, (100), (110), (111) and (112) were measured. Subsequently the ODF was estimated using an academic software MTM-FHM [47].

3.2.2 Micro Texture

A Fei-quanta SEM (scanning electron microscope) attached with TSL-OIM was used for micro-texture characterization [48]. The system is known as electron backscattered diffraction (EBSD) system. This is also available at IIT Bombay and is used for the present study. EBSD was carried out for grain size and grain average misorientation determination. Grain average misorientation (GAM) is the average misorientation between each point in a grain.

3.3 Magnetic Properties

Various magnetic properties were measured by equipment called PC based Pulse Field Hysteresis Loop Tester. It is used for quick characterization of magnetic materials at room temperature. High magnetic field is generated in a solenoid by passing through it, a pulse current of sinusoidal shape at an interval which is slow enough to produce minimum heating as per the specification in the solenoid. A pickup coil system is kept in the proximity of a solenoid to detect field and magnetization signal of a sample placed in the pickup coil. These transitory analog signals are basically converted into digital signals by a micro-controller integrated circuit. A software used to interface the system to the PC and datas are processed to calculate various hysteresis parameters like saturation magnetization M_s, coercivity H_c, followed by plotting of the hysteresis loop (M Vs H curve)[49]. From the Graph χ_m (susceptibility by mass) was obtained by the relation:

$$M = \chi_m H$$

Again from χ_m permeability can be measure by the following form

$$\mu = \mu_0 (1+\chi_m)$$

Where, μ= absolute permeability of sample

μ_0= permeability of air, χ_m= susceptibility by mass

3.4 Electrical Property

The electrical resistivity of each CRNO steel samples were measured by calculating resistance in electrical laboratory by four probe method. From the electrical resistances of different samples the resistivities were subsequently calculated and the eddy current loss can be determined by using the following formulae:

Electrical resistivity = $(\pi tR/\ln 2)$ (if t<< length, as in this case)

Classical eddy current loss = $(10^{-13}\pi^2 t^2 B^2 f^2)/(6\rho\sigma)$

Where, 't' is the thickness in cm, 'B', the induction in Gauss f, the frequency in Hz , ρ, is the specific density in g/cm^3 σ, is the resistivity in ohm.cm and the core loss estimated in watts/kg.

CHAPTER IV

4.0 Results and Discussions

The inverse pole figure maps of CRNO samples in the rolling direction is shown in Figure 4.1. The black regions in the figure indicate low confidence index (<0.5). Confidence index determines the accuracy in detecting the diffraction pattern. In general for highly deformed regions the confidence index is always low because of distorted kikuchi diffraction pattern. Hence, it may be conclude that the samples were not fully annealed condition. Further as shown in Figure 4.2 the average grain average misorientation values are higher (>1.5); also support the earlier statement. For a fully annealed/recrystallized material the average grain average misorientaion is less than/equal to 0.5. The average grain size is approximately equal in all CRNO samples. Figure 4.1 also shows that the material is textured in <111> and <001> orientations. However, the EBSD micro-texture is statistically poor compared to XRD bulk texture. Figures 4.3-4.6 show the ODFs of different CRNO samples examined in the present study. This includes ODFs of all CRNO samples (Figure 4.3: A1-0, A1-30, A1-60, A1-90; Figure 4.4: A2-0, A2-30, A2-60, A2-90; Figure 4.5:A3-0, A3-30, A3-60, A3-90 and Figure 4.6: A4-0, A4-30, A4-60, A4-90). It may be noted that the EBSD measurements were carried out only in the rolling directions because EBSD was used to investigate the microstructural/grain size developments only and this may be expected to be similar in all angular directions.

As shown in figures 4.3-4.6 the texture in the rolling direction is much higher compared to other angular directions. The maximum ODF intensity of all CRNO samples is shown in Figure 4.7. Maximum ODF intensity indicates the amount of texturing in a sample – higher the value indicates the better texture. From magnetic properties point of view the Goss and Cube orientations are important. Table 4.1 shows the volume fraction of Goss and Cube orientations in all CRNO samples examined in the present study. Apart from Goss and Cube orientations, other important texture i.e. alpha, gamma and theta fibers volume fractions have also been reported. As shown in table 4.1, the volume fraction of Goss orientation is higher in rolling direction compared to other angular directions in all CRNO samples whereas the reverse trend is valid in case of cube volume fractions.

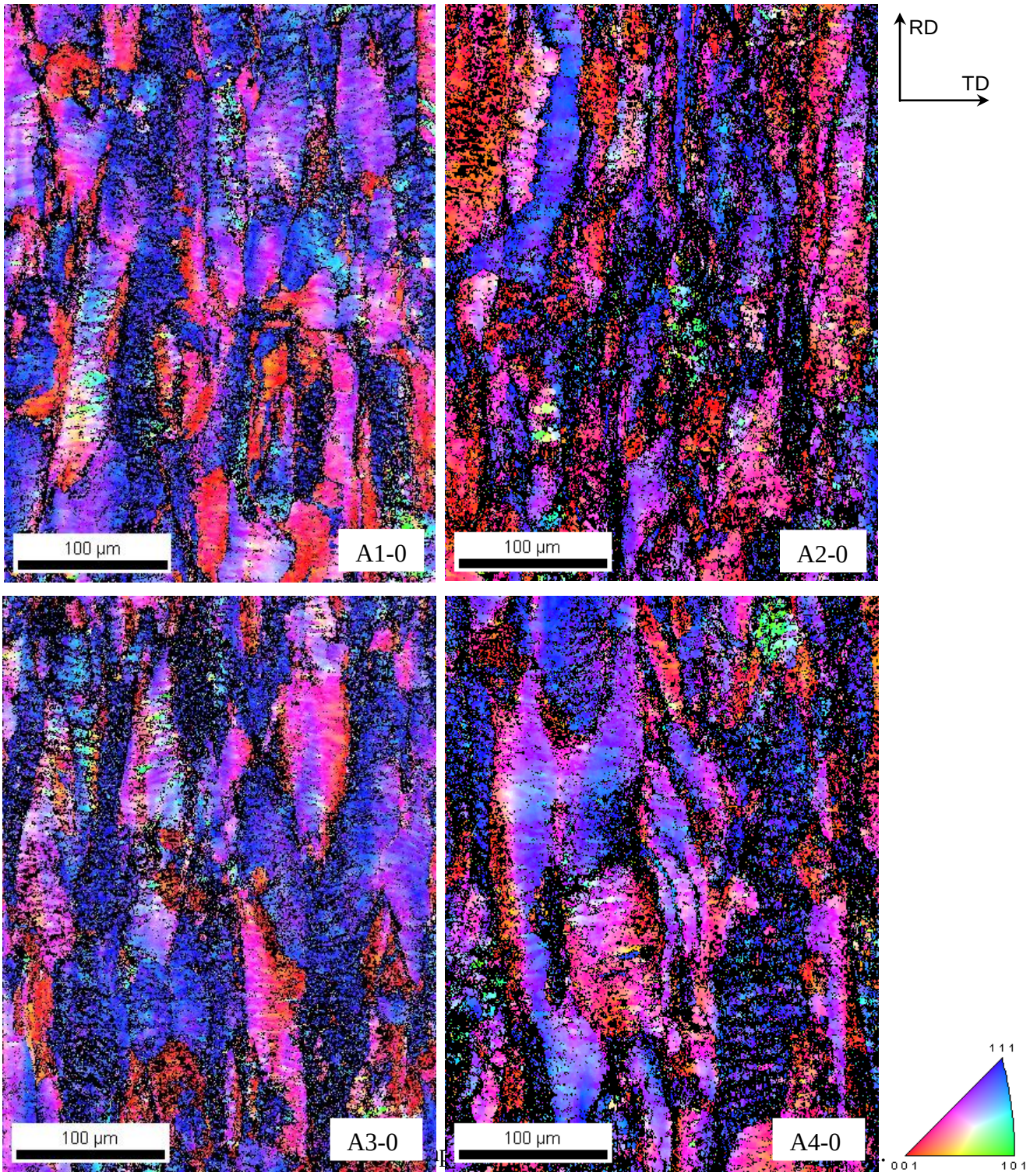

Fig. 4.1. Inverse pole figure maps of CRNO samples in the rolling direction.

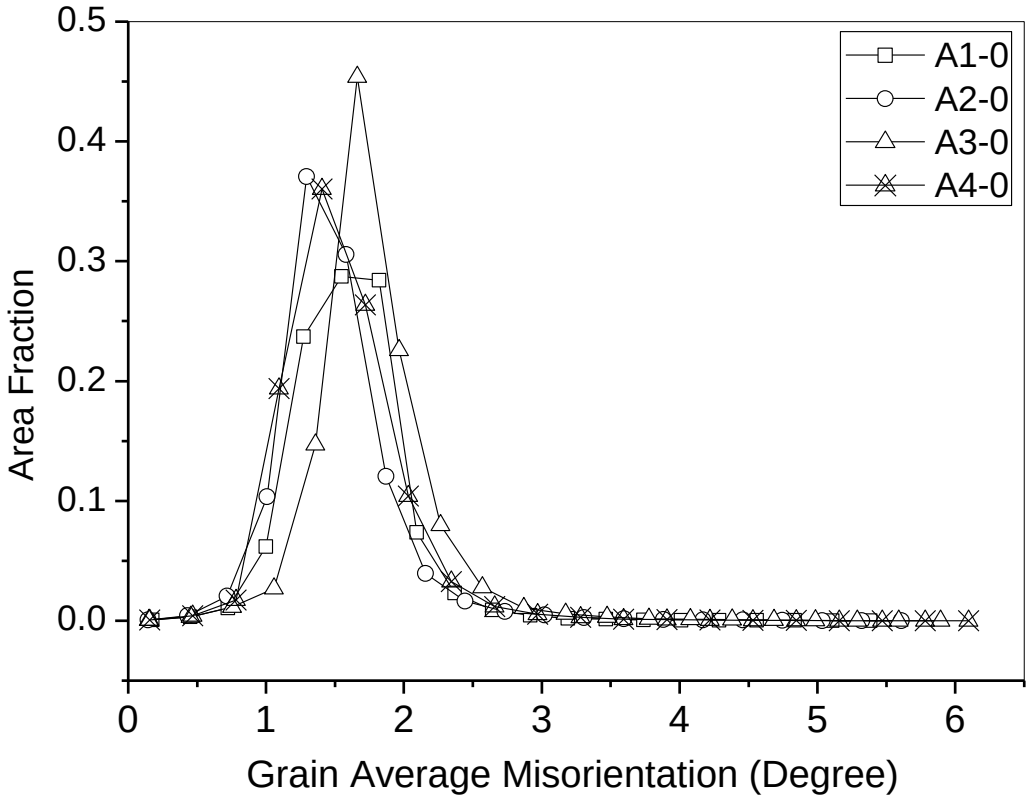

Figure 4.2. Grain average misorientation (GAM) of the EBSD scans shown in figure 4.1.

Samples	ODFs
A1-0	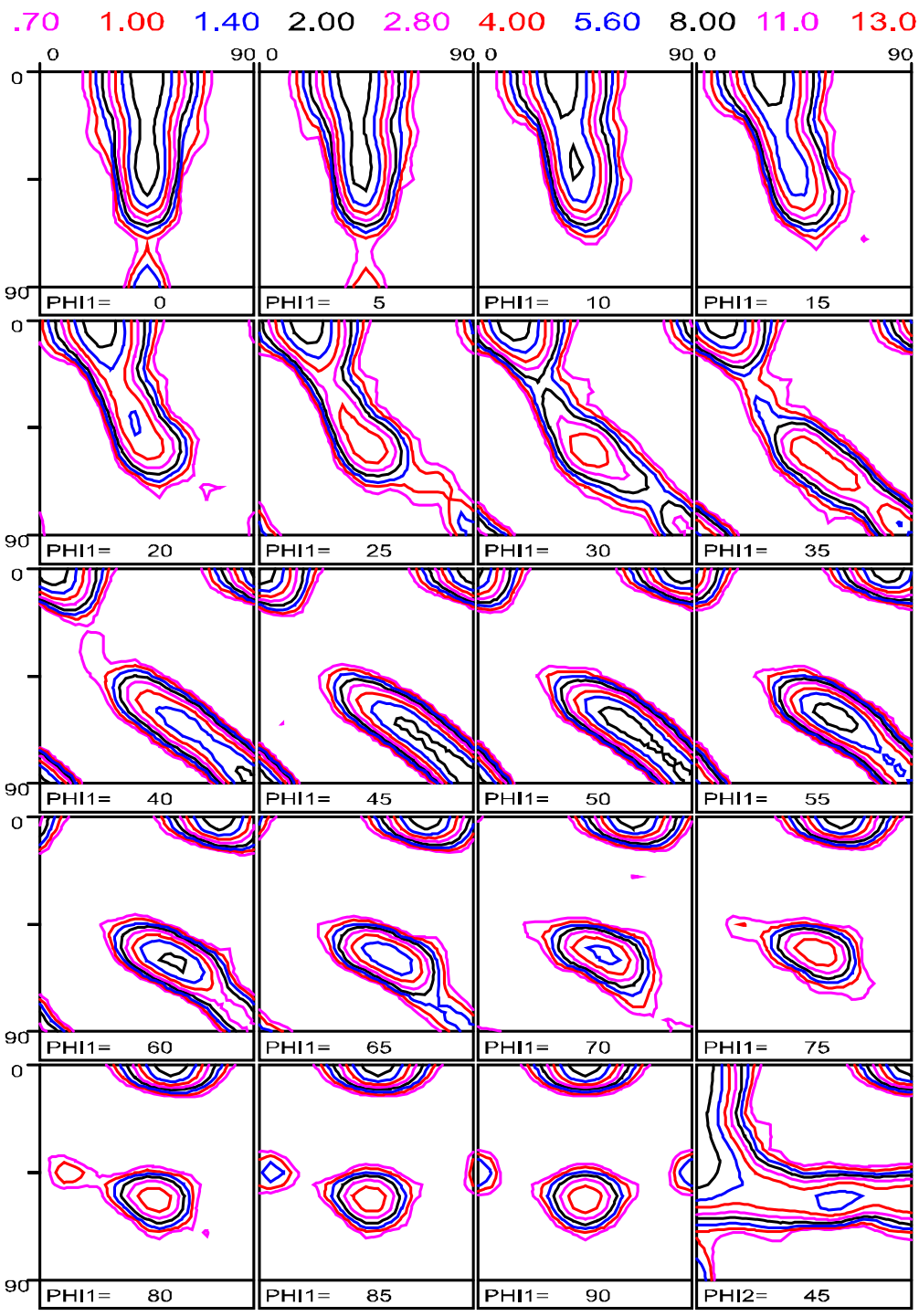

A2-0	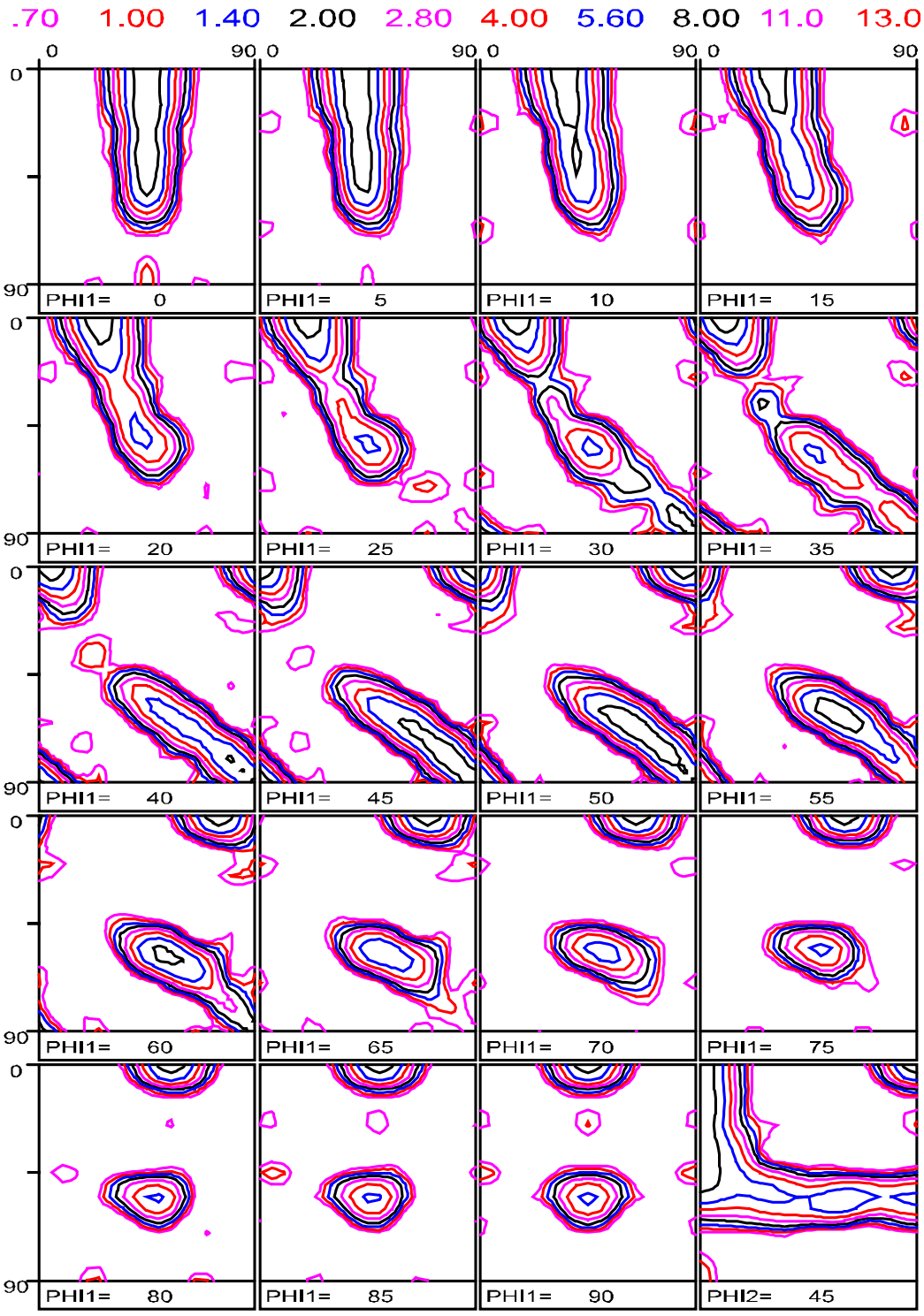 .70 1.00 1.40 2.00 2.80 4.00 5.60 8.00 11.0 13.0 0 90 0 90 0 90 0 90 0 90 PHI1= 0 PHI1= 5 PHI1= 10 PHI1= 15 PHI1= 20 PHI1= 25 PHI1= 30 PHI1= 35 PHI1= 40 PHI1= 45 PHI1= 50 PHI1= 55 PHI1= 60 PHI1= 65 PHI1= 70 PHI1= 75 PHI1= 80 PHI1= 85 PHI1= 90 PHI2= 45

A3-0

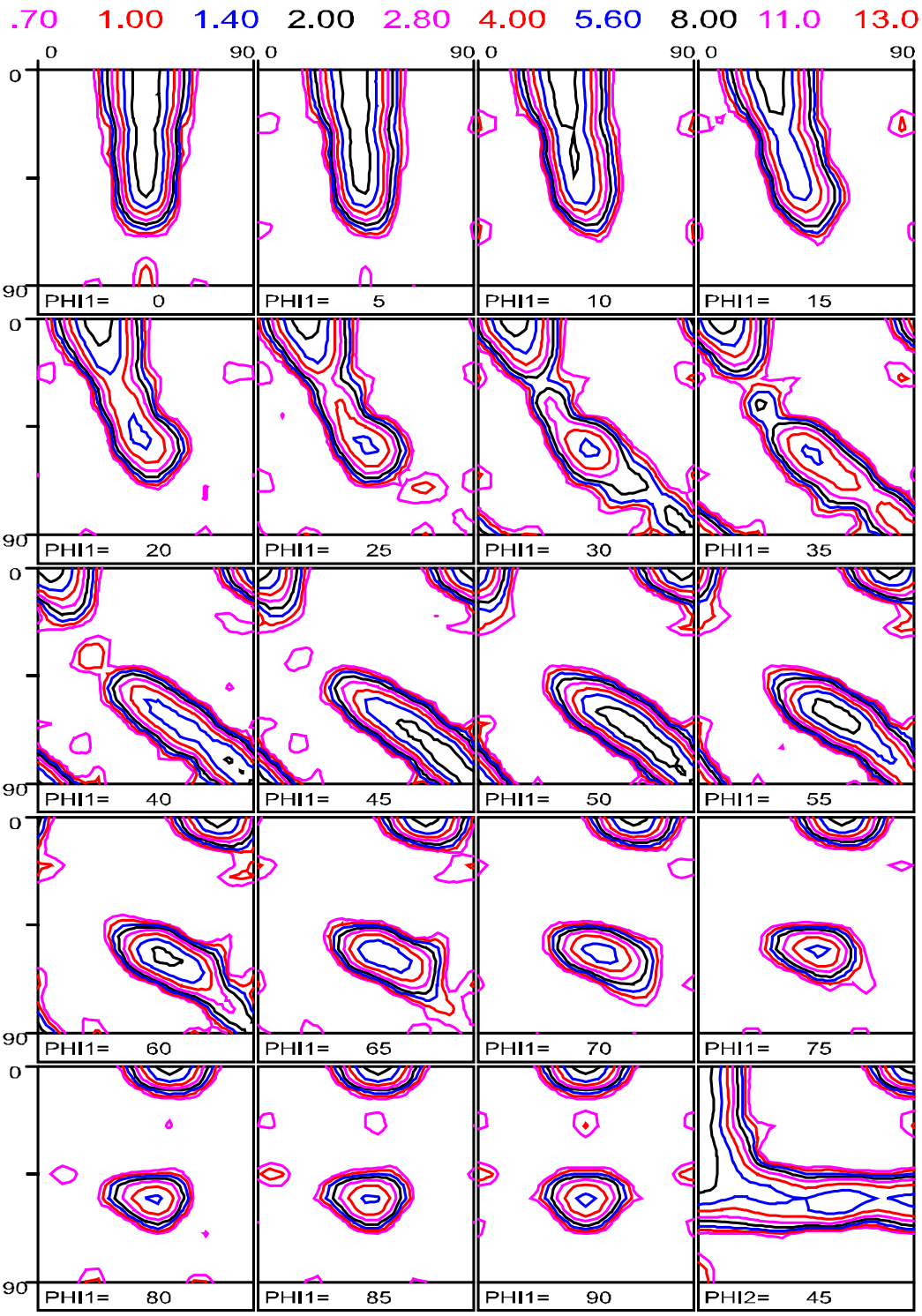
.70 1.00 1.40 2.00 2.80 4.00 5.60 8.00 11.0 13.0
0 90
PHI1= 0
PHI1= 5
PHI1= 10
PHI1= 15
PHI1= 20
PHI1= 25
PHI1= 30
PHI1= 35
PHI1= 40
PHI1= 45
PHI1= 50
PHI1= 55
PHI1= 60
PHI1= 65
PHI1= 70
PHI1= 75
PHI1= 80
PHI1= 85
PHI1= 90
PHI2= 45

A4-0

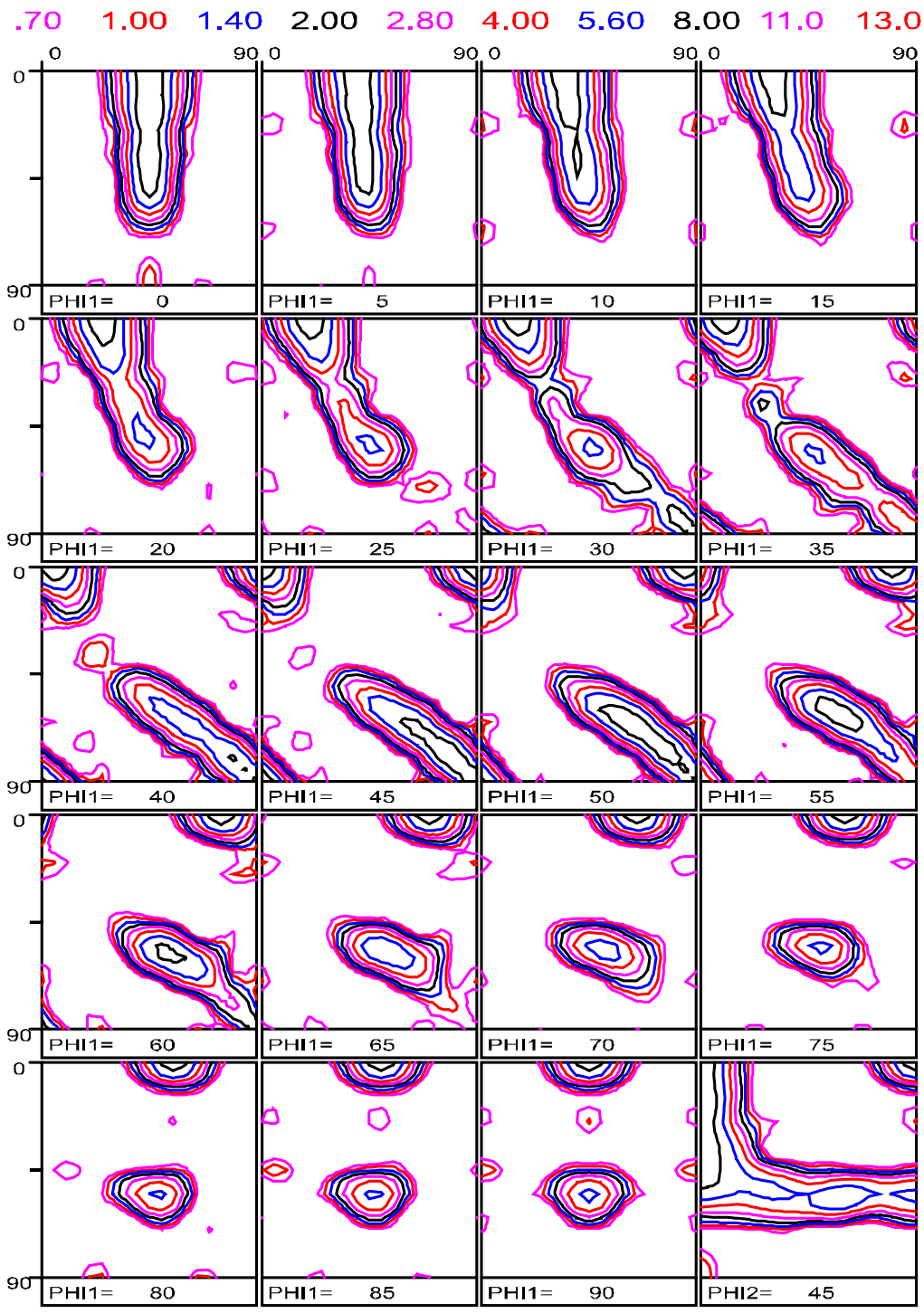

Figure 4.3. ODFs of different CRNO samples in the rolling direction (at constant φ_1 sections and a constant φ_2=45° section)

Samples	ODFs
A1-30	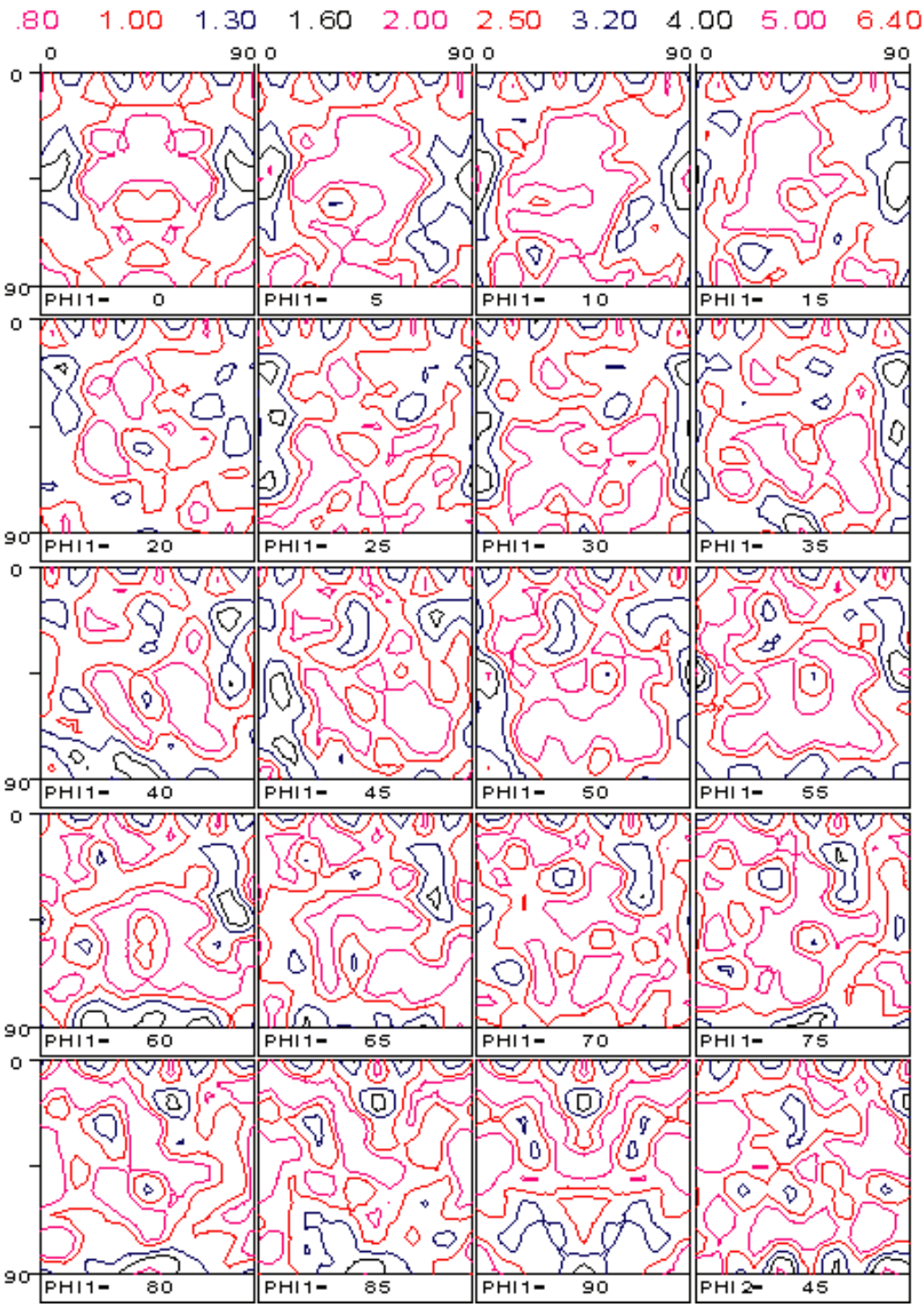

A2-30

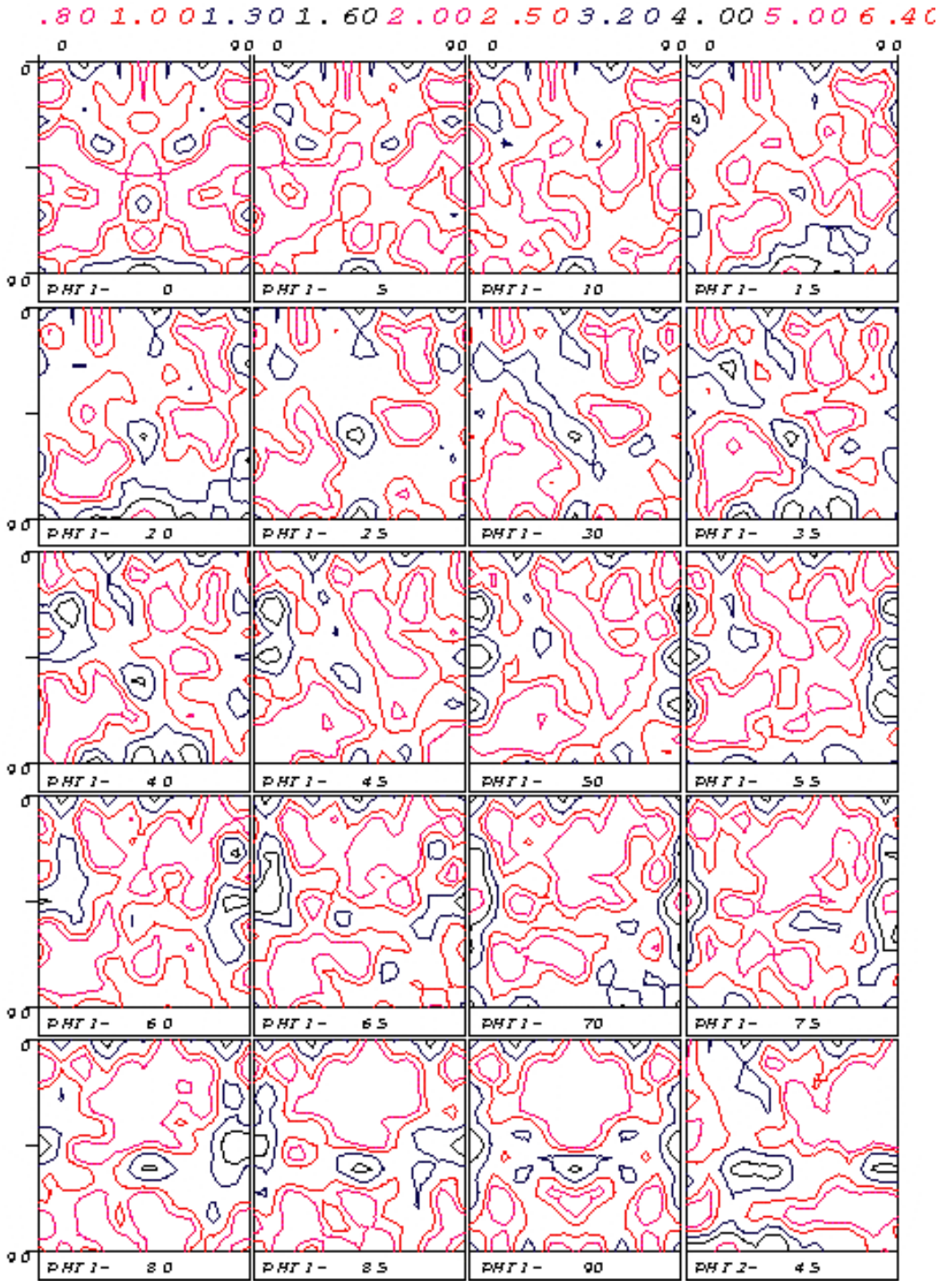
.80 1.00 1.30 1.60 2.00 2.50 3.20 4.00 5.00 6.40
0 90
PHI1- 0
PHI1- 5
PHI1- 10
PHI1- 15
PHI1- 20
PHI1- 25
PHI1- 30
PHI1- 35
PHI1- 40
PHI1- 45
PHI1- 50
PHI1- 55
PHI1- 60
PHI1- 65
PHI1- 70
PHI1- 75
PHI1- 80
PHI1- 85
PHI1- 90
PHI2- 45

A3-30

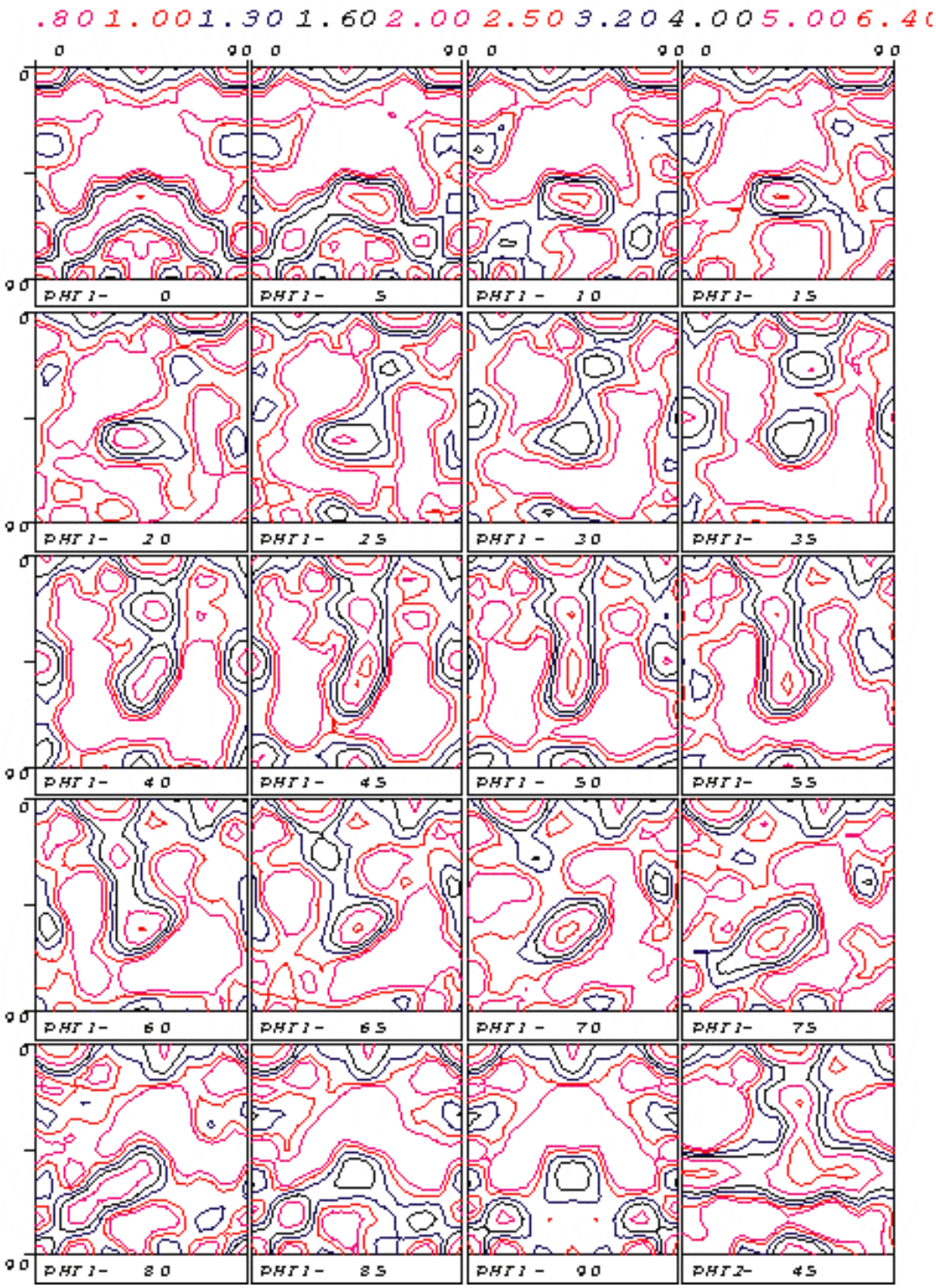
.80 1.00 1.30 1.60 2.00 2.50 3.20 4.00 5.00 6.40
PHI1- 0
PHI1- 5
PHI1- 10
PHI1- 15
PHI1- 20
PHI1- 25
PHI1- 30
PHI1- 35
PHI1- 40
PHI1- 45
PHI1- 50
PHI1- 55
PHI1- 60
PHI1- 65
PHI1- 70
PHI1- 75
PHI1- 80
PHI1- 85
PHI1- 90
PHI2- 45

A4-30

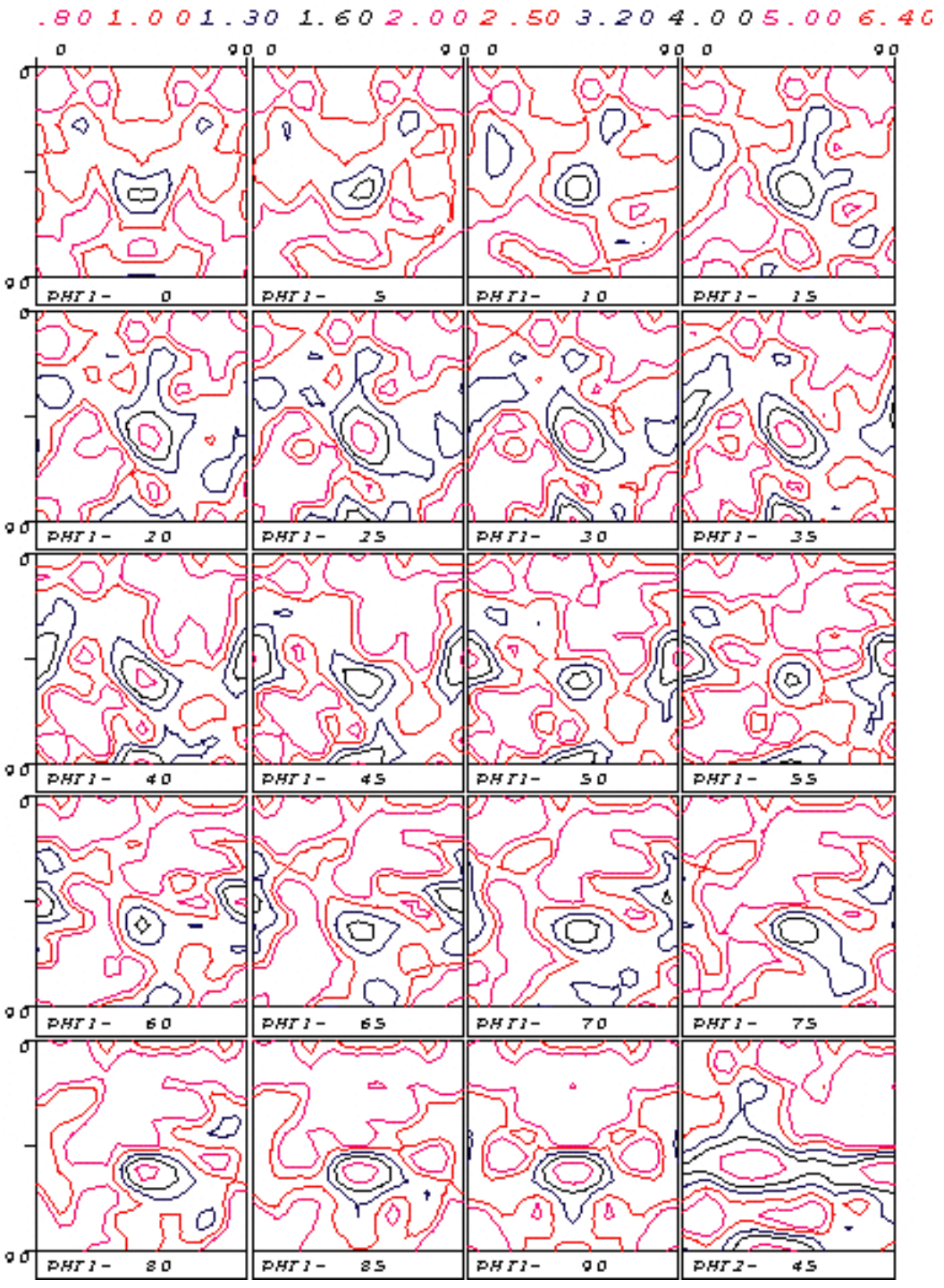

Figure 4.4. ODFs of different CRNO samples at 30° to the rolling direction (at constant φ_1 sections and a constant φ_2=45° section).

Samples	ODFs
A1-60	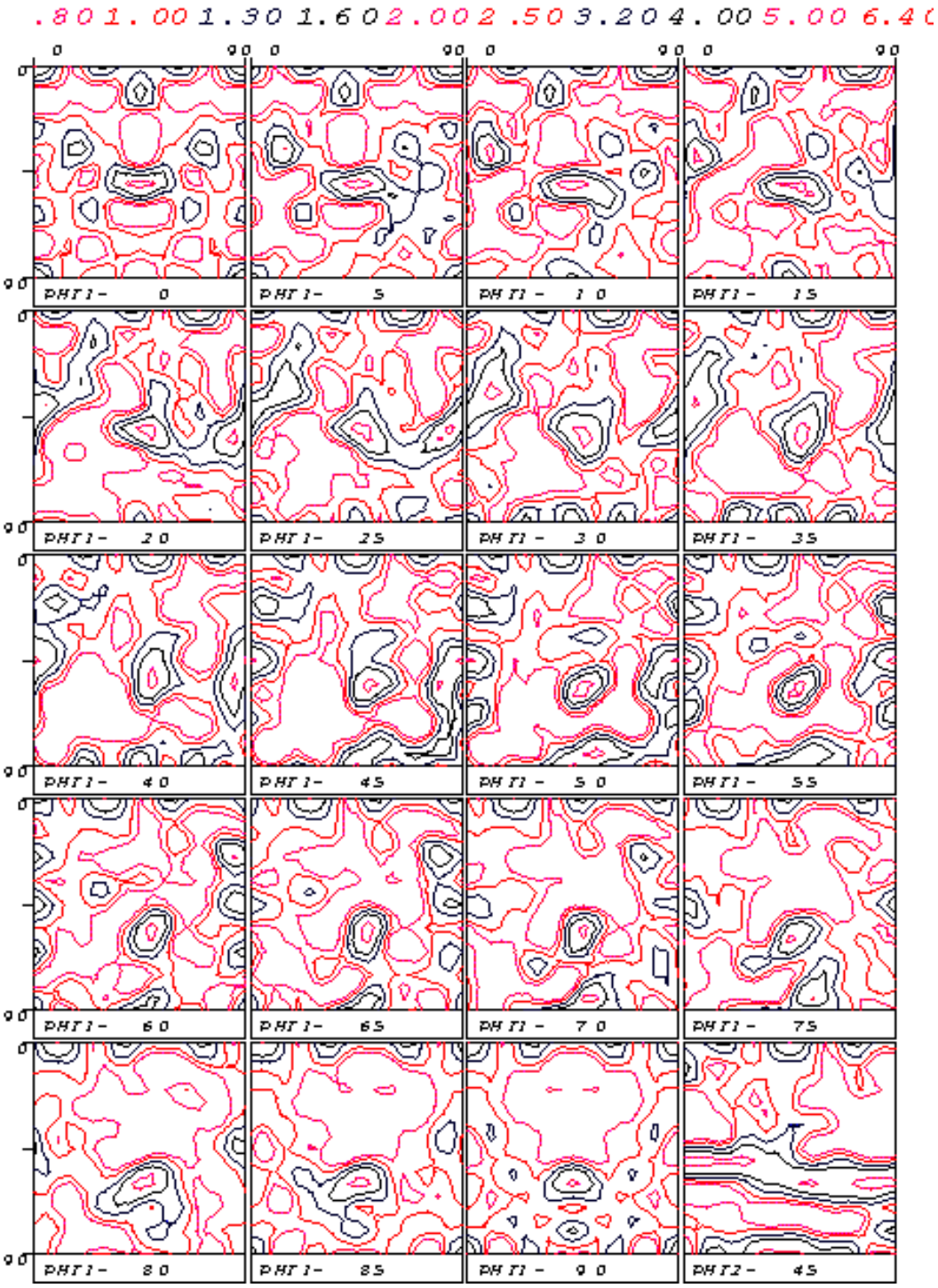

A2-60

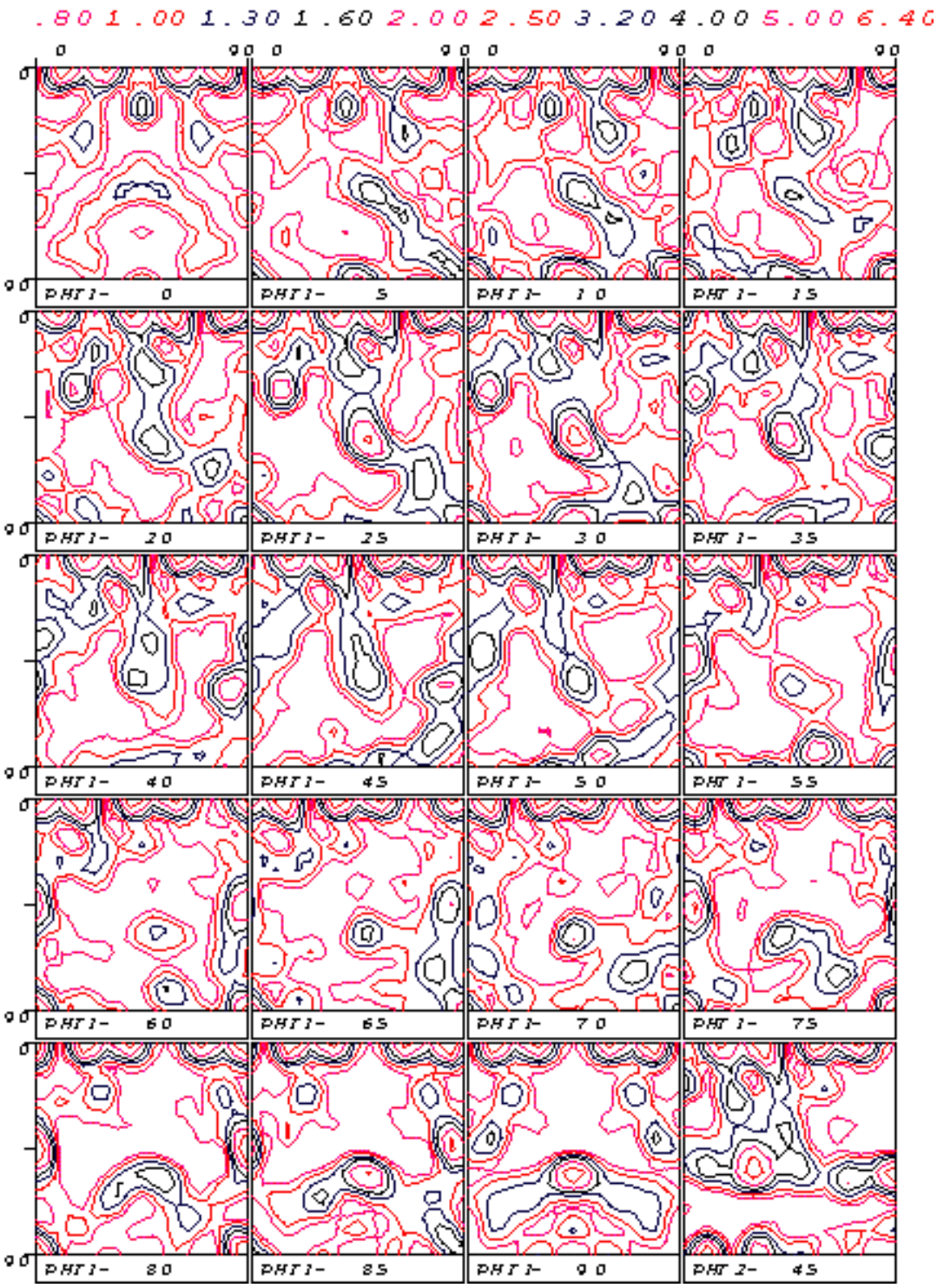
.80 1.00 1.30 1.60 2.00 2.50 3.20 4.00 5.00 6.40
PHI1- 0
PHI1- 5
PHI1- 10
PHI1- 15
PHI1- 20
PHI1- 25
PHI1- 30
PHI1- 35
PHI1- 40
PHI1- 45
PHI1- 50
PHI1- 55
PHI1- 60
PHI1- 65
PHI1- 70
PHI1- 75
PHI1- 80
PHI1- 85
PHI1- 90
PHI2- 45

A3-60

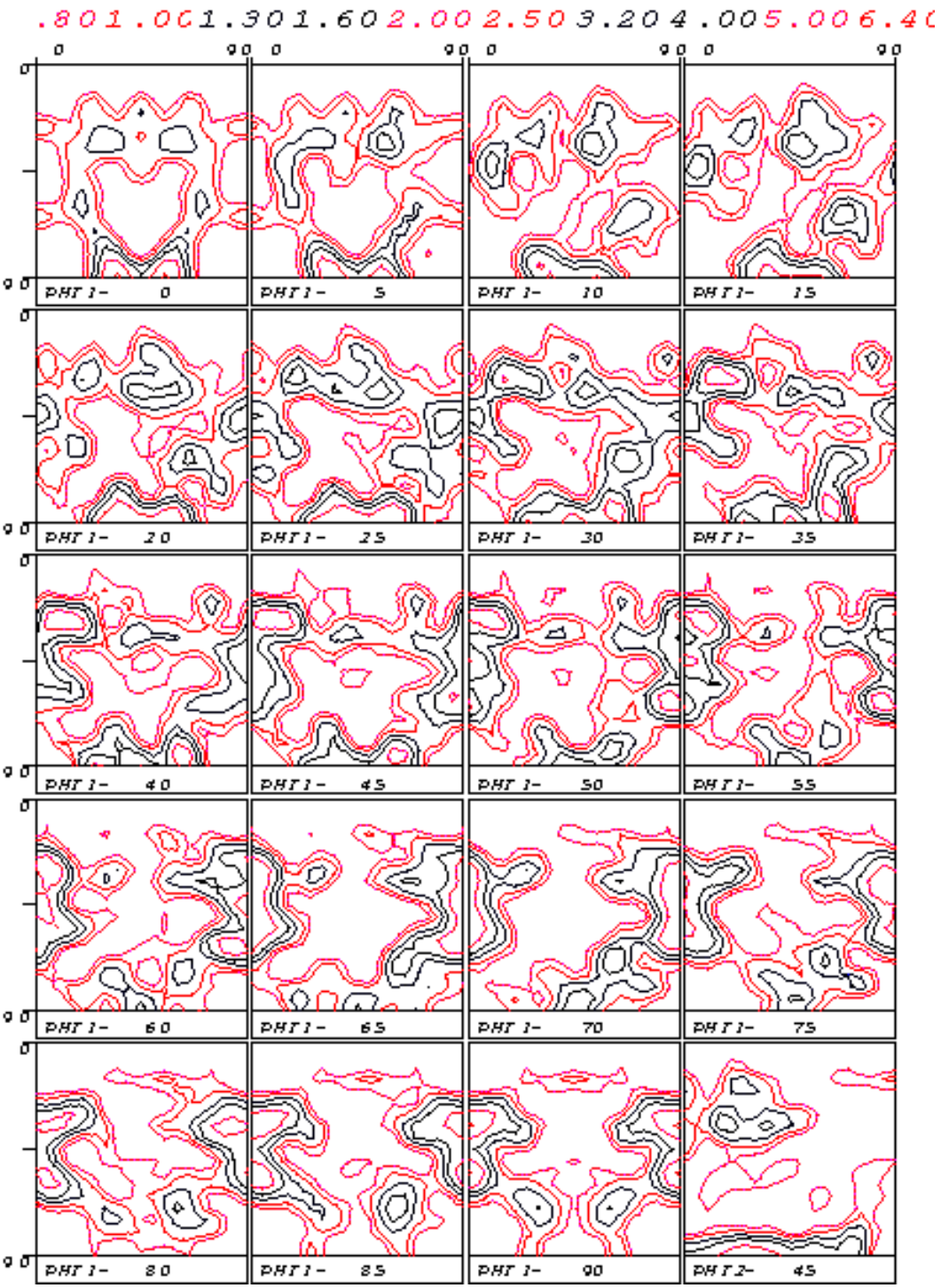
.801.001.301.602.002.503.204.005.006.40
0
90
PHI1- 0
PHI1- 5
PHI1- 10
PHI1- 15
PHI1- 20
PHI1- 25
PHI1- 30
PHI1- 35
PHI1- 40
PHI1- 45
PHI1- 50
PHI1- 55
PHI1- 60
PHI1- 65
PHI1- 70
PHI1- 75
PHI1- 80
PHI1- 85
PHI1- 90
PHI2- 45

A4-60

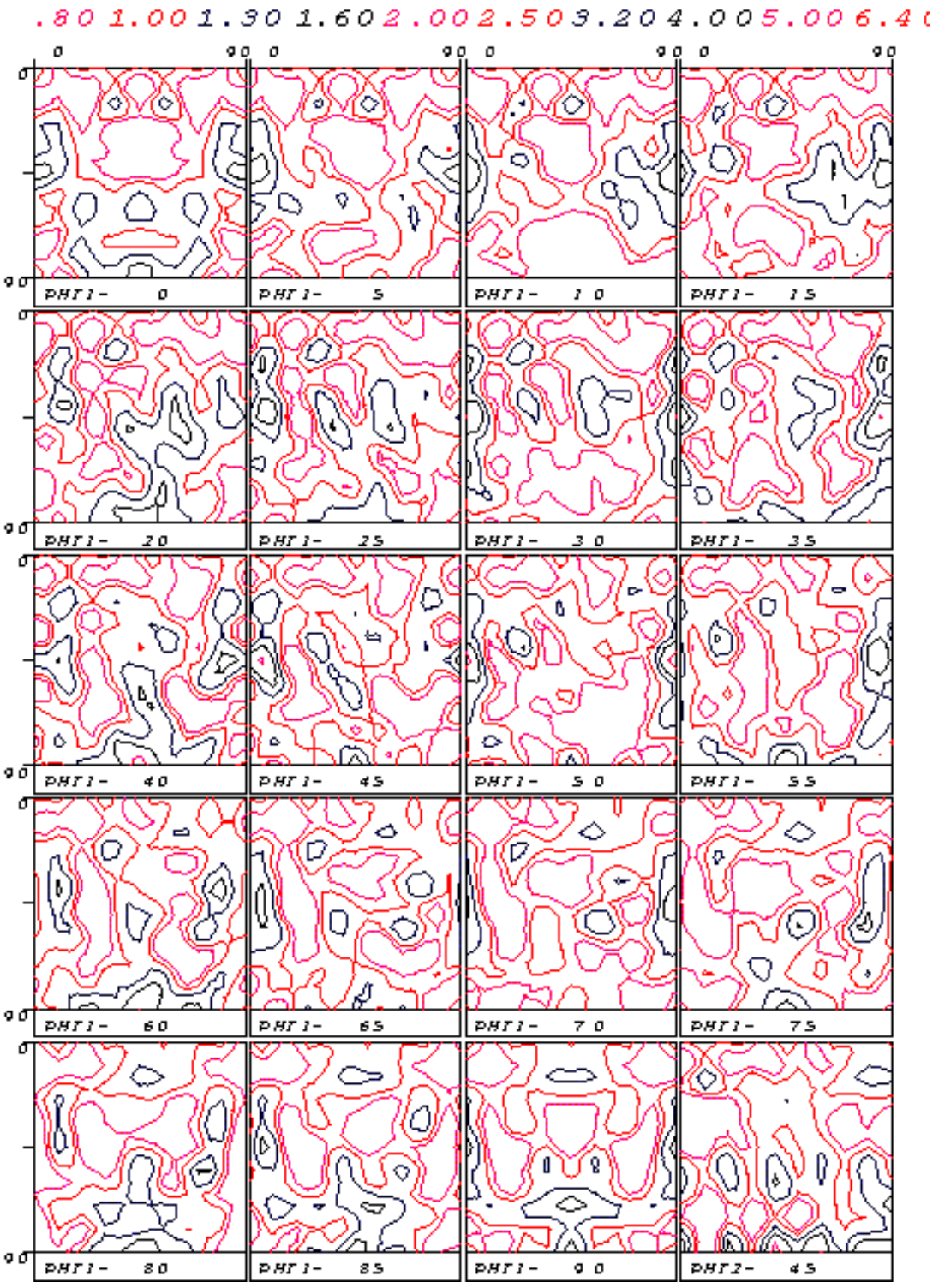

Figure 4.5. ODFs of different CRNO samples at 60° to the rolling direction (at constant φ_1 sections and a constant φ_2=45° section).

Samples	ODFs
A1-90	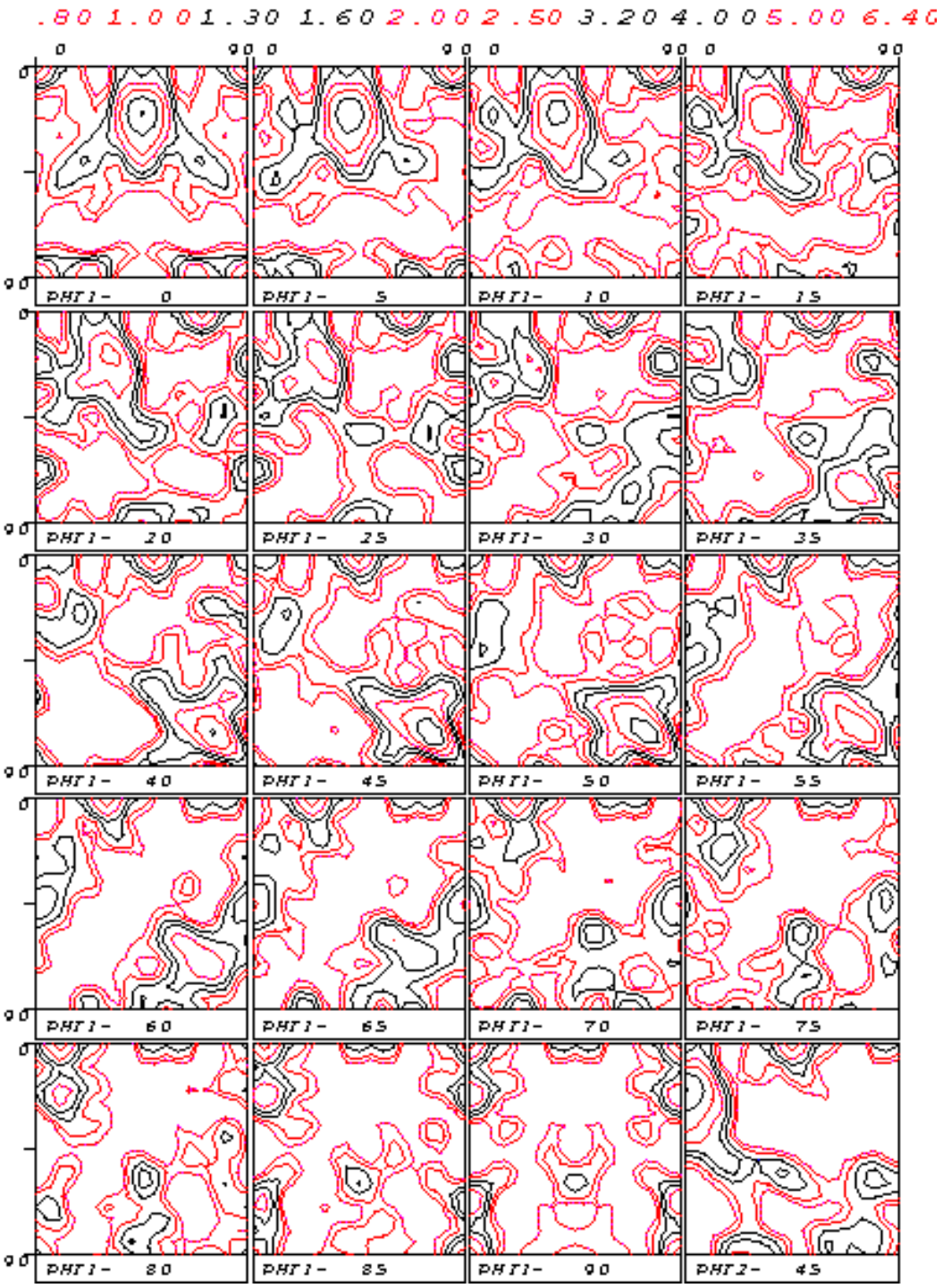

A2-90

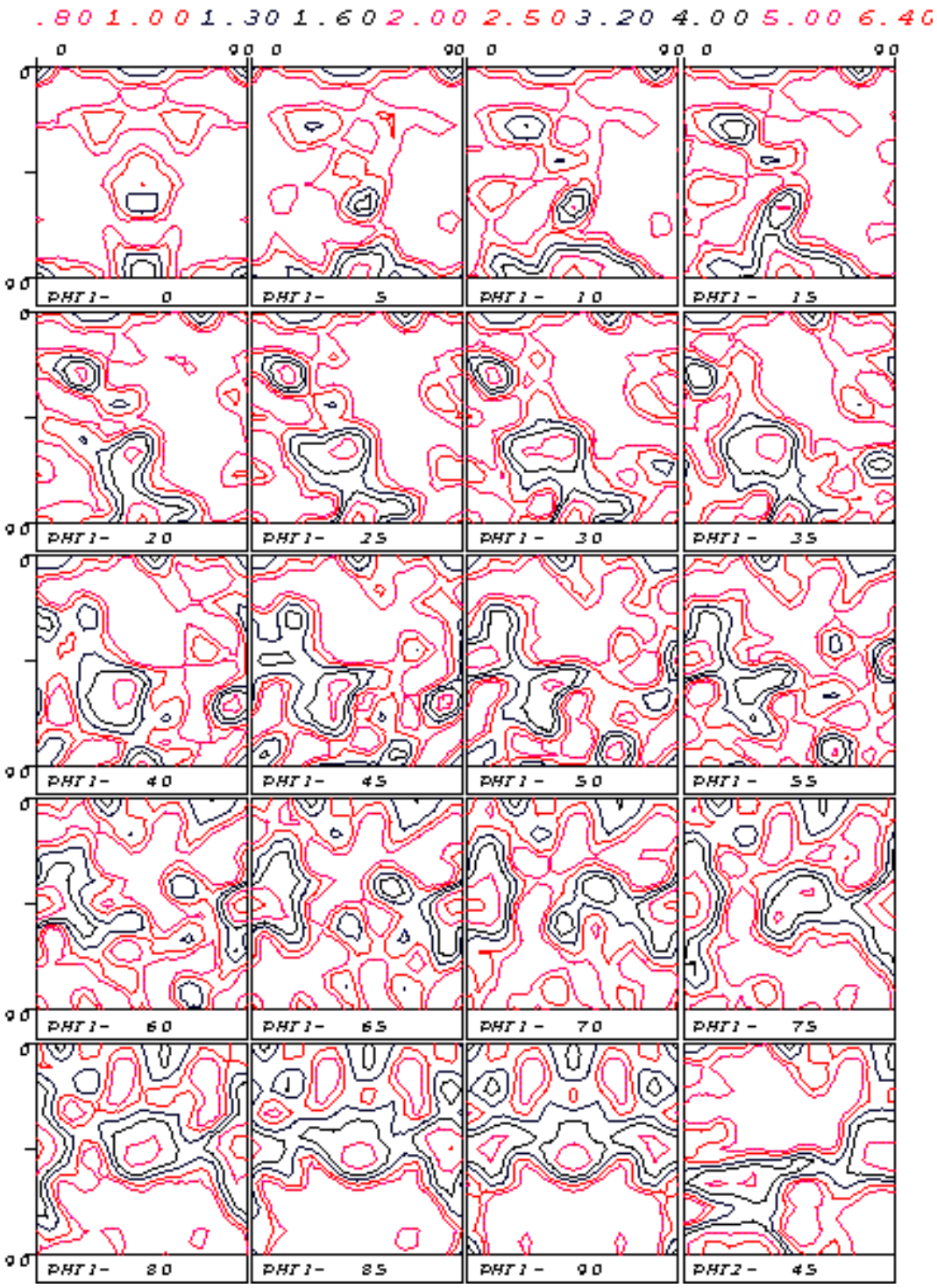
.80 1.00 1.30 1.60 2.00 2.50 3.20 4.00 5.00 6.40
PHI1- 0
PHI1- 5
PHI1- 10
PHI1- 15
PHI1- 20
PHI1- 25
PHI1- 30
PHI1- 35
PHI1- 40
PHI1- 45
PHI1- 50
PHI1- 55
PHI1- 60
PHI1- 65
PHI1- 70
PHI1- 75
PHI1- 80
PHI1- 85
PHI1- 90
PHI2- 45

A3-90

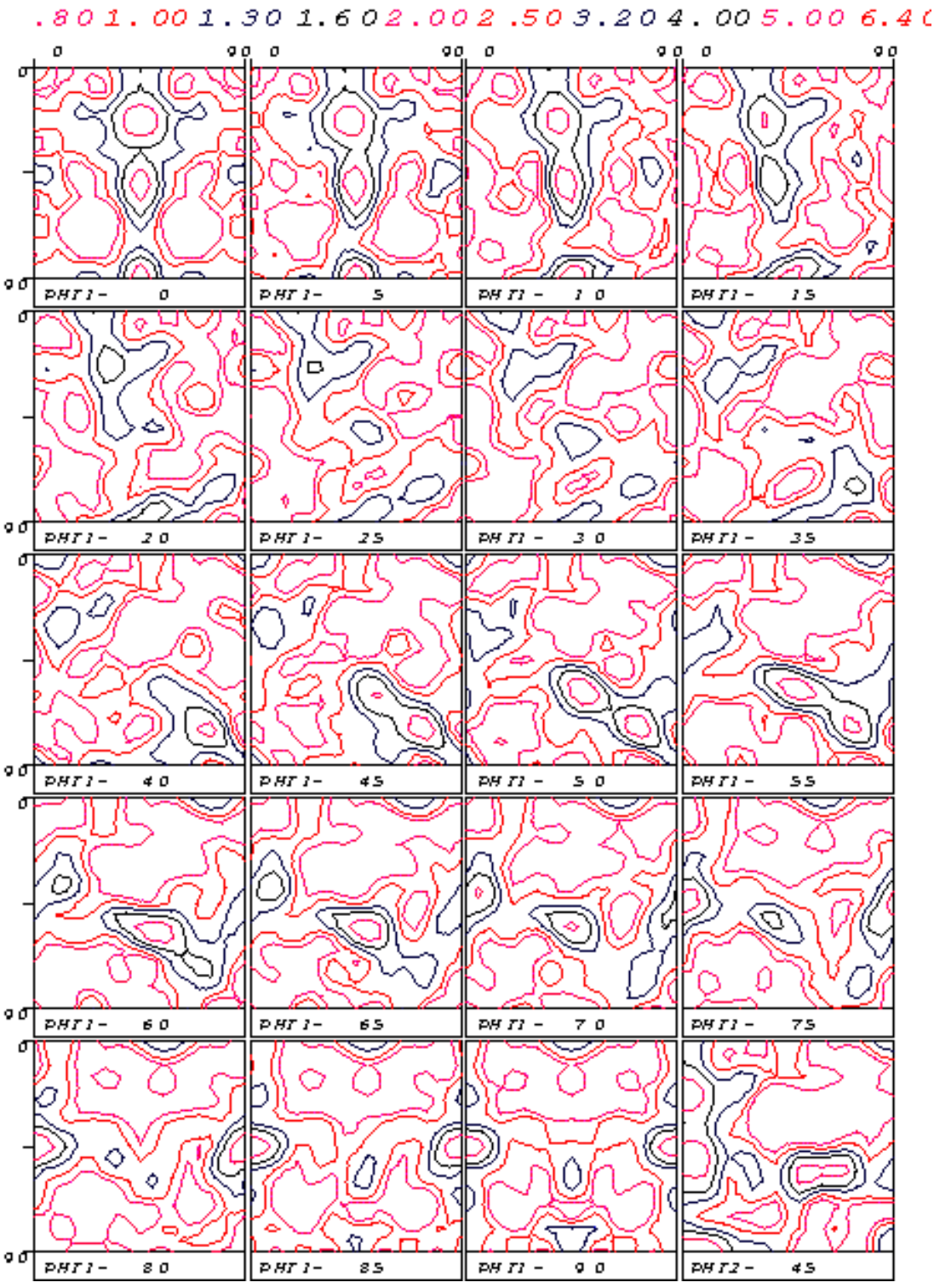
.80 1.00 1.30 1.60 2.00 2.50 3.20 4.00 5.00 6.40
0 90
PHI1- 0
PHI1- 5
PHI1- 10
PHI1- 15
PHI1- 20
PHI1- 25
PHI1- 30
PHI1- 35
PHI1- 40
PHI1- 45
PHI1- 50
PHI1- 55
PHI1- 60
PHI1- 65
PHI1- 70
PHI1- 75
PHI1- 80
PHI1- 85
PHI1- 90
PHI2- 45

A4-90

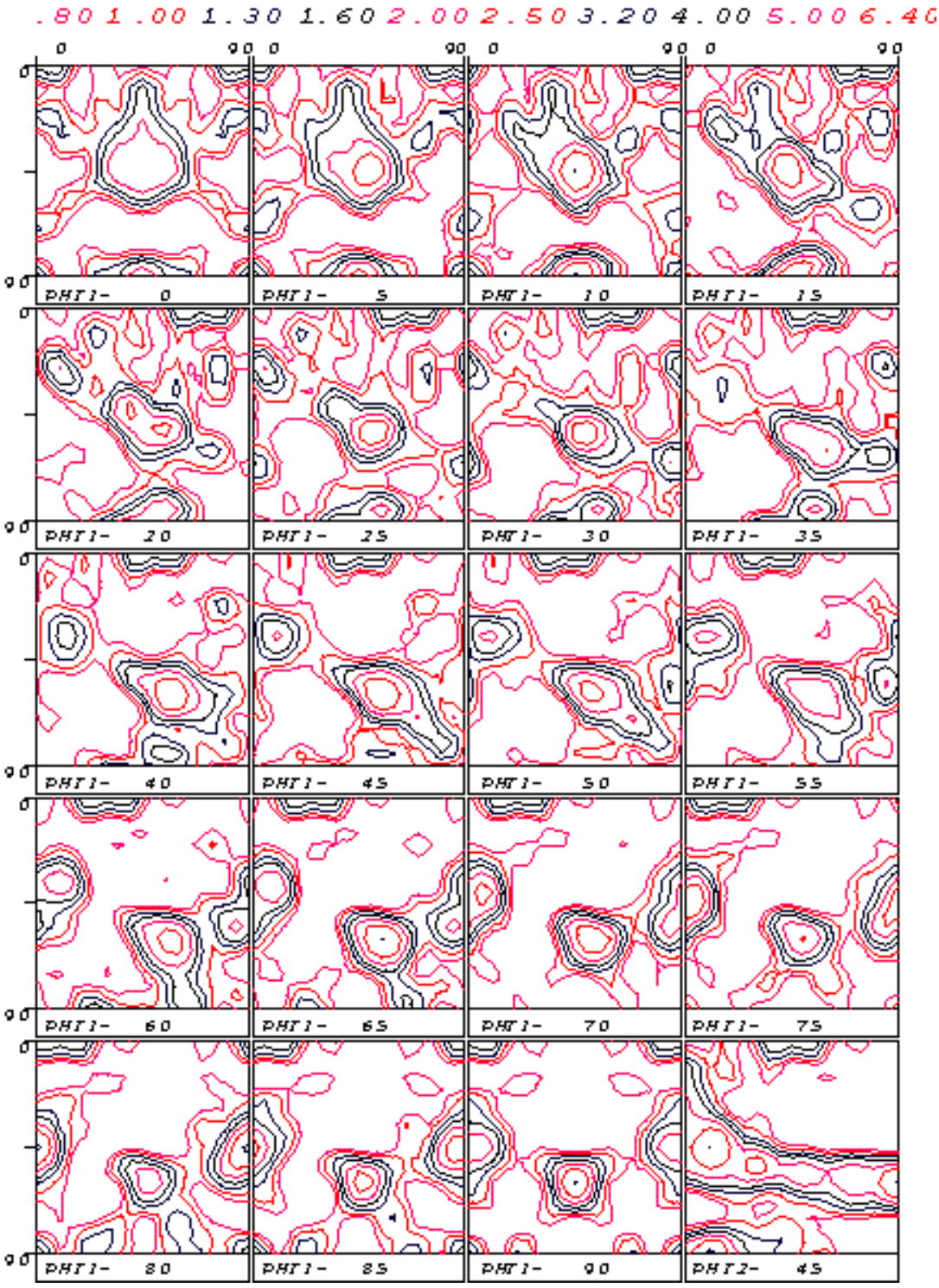

Figure 4.6. ODFs of different CRNO samples at 90° to the rolling direction (at constant φ_1 sections and a constant φ_2=45° section).

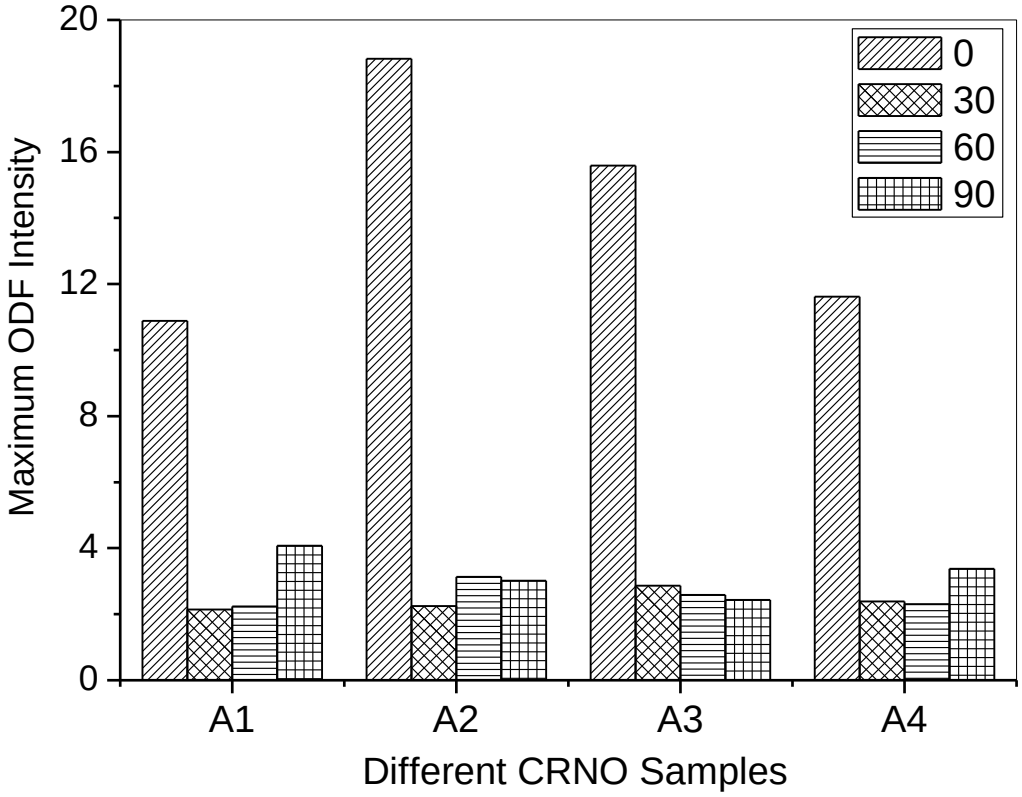

Figure 4.7. Maximum ODF intensity of different CRNO samples.

Table 4.1. Volume fraction of important orientations in the present CRNO samples. The highlighted orientations i.e. Goss and Cube are compared for the present study – these two decide the magnetic properties of a material.

(hkl)<uvw>	A1-0	A1-30	A1-60	A1-90	A2-0	A2-30	A2-60	A2-90	A3-0	A3-30	A3-60	A3-90	A4-0	A4-30	A4-60	A4-90
(110)<uvw> Alpha Fiber	0.5192	0.1447	0.1586	0.1803	0.5245	0.1585	0.1555	0.1666	0.5245	0.1539	0.1510	0.1847	0.5245	0.1598	0.1463	0.1838
(111)<uvw> Gamma Fiber	0.3376	0.1445	0.1775	0.1553	0.3545	0.1625	0.1656	0.1791	0.3545	0.2005	0.1356	0.1835	0.3545	0.1925	0.1641	0.2082
(001)<uvw> Theta Fiber	0.1644	0.1264	0.1166	0.1275	0.1476	0.1198	0.1388	0.1071	0.1476	0.1345	0.0871	0.1115	0.1476	0.0998	0.1118	0.1007
(110)<100> Goss Orientation	0.0144	0.0504	0.04354	0.0400	0.0116	0.0346	0.03606	0.0266	0.0116	0.03999	0.03712	0.03737	0.01159	0.03892	0.04972	0.03471
(100)<001> Cube Orientation	0.05465	0.03893	0.03843	0.04314	0.06286	0.03778	0.04547	0.03383	0.06286	0.05158	0.02576	0.03586	0.06286	0.02960	0.03357	0.03363

Figure 4.8 shows the increase is resistivity with increase in Si percentages of CRNO steels used in the present study. The magnetic permeability and eddy current loss of different CRNO samples is represented in table 4.2. The CRNO samples in the rolling direction had shown high permeability and low eddy current loss with highest texture development. As shown in Figure 4.9 the sample A2-0 had highest textural development among all the samples and it had high permeability and low eddy current loss. Other samples i.e. samples other than rolling direction had insignificant texture developments and didn't show any link/trend between texture and magnetic properties.

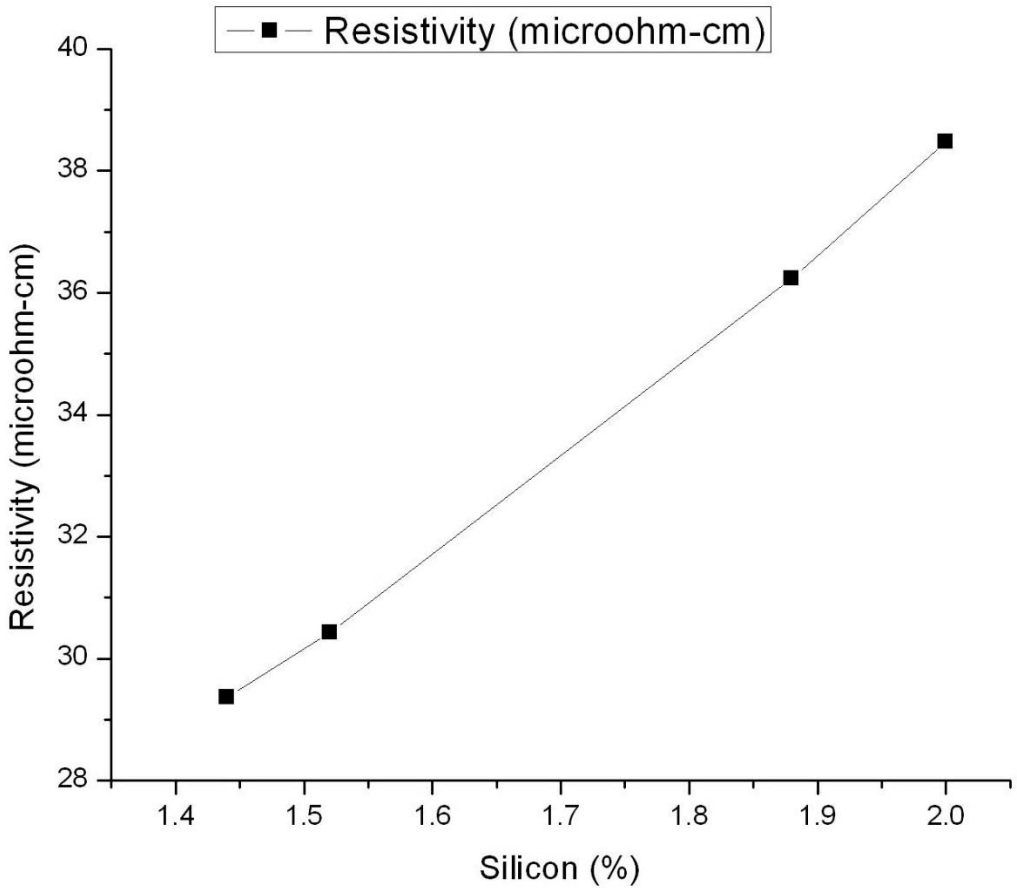

Figure 4.8. Variation of resistivity with increase in Si percentages of CRNO steels.

Table 4.2. Experimental results on electrical and magnetic properties of CRNO samples used in the present study.

Samples	Resistivity(micro ohm-cm)	Permeability	Saturation Induction(B_s)(T)	Eddy current loss (watts/kg)
A1-0	38.48	1295	0.780	0.202
A1-30	38.48	1262	0.805	0.218
A1-60	38.48	1345	0.831	0.233
A1-90	38.48	1310	0.824	0.228
A2-0	36.24	1333	0.797	0.227
A2-30	36.24	1320	0.847	0.257
A2-60	36.24	1312	0.813	0.234
A2-90	36.24	1279	0.793	0.224
A3-0	30.43	1303	0.800	0.271
A3-30	30.43	1325	0.895	0.305
A3-60	30.43	1283	0.781	0.261
A3-90	30.43	1306	0.832	0.296
A4-0	29.37	1303	0.801	0.281
A4-30	29.37	1330	0.828	0.301
A4-60	29.37	1303	0.828	0.301
A4-90	29.37	1298	0.817	0.296

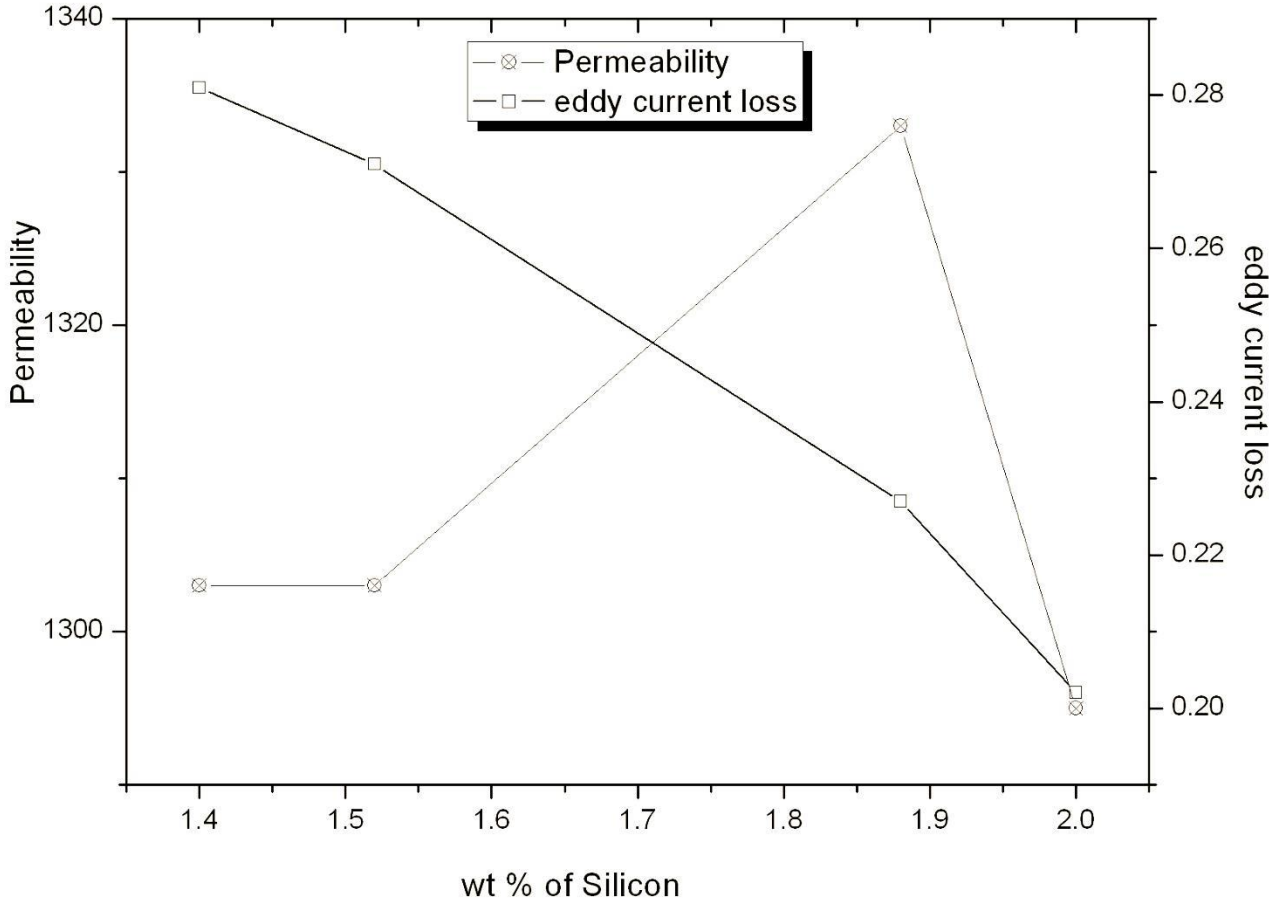

Figure 4.9. Variation of permeability and eddy current loss with silicon percentages of CRNO steels in the rolling direction.

CHAPTER V

5.0 Summary

Texture and magnetic properties of four CRNO steel sheets of different Si percentages (2%, 1.88%, 1.52% and 1.4%) in rolling direction, 30° to the rolling direction, 60° to the rolling direction and 90° to the rolling direction were investigated in the present study. The following conclusions are made:

- Textural development in CRNO steels is independent of Si percentages. However, it is strongly dependent on angular orientation of CRNO sheets – texture development is higher in rolling direction compared to other angular directions.
- The electrical resistivity increases with increase in Si percentages. However, the magnetic permeability and eddy current loss didn't show any trend with composition i.e. variation of Si percentages.
- The sample with highest texture had high permeability and low eddy current loss.
- The samples other than rolling direction had insignificant texture developments and didn't show any link/trend between texture and magnetic properties.

5.1 Scope for Further Work

In the present study we found that texture had strong influence on magnetic properties of CRNO steels. Also texture is highly dependent on processing parameters. Hence, it may be tried to improve the texture in all angular directions of CRNO sheets so that the magnetic properties will be uniform in all directions. This may be achieved by cross rolling and subsequent heat treatments. As it is well known that the texture developments in CRNO steels mostly occur during hot/cold rolling.

6.0 References

1. M. Matsuo, ISIJ Int. 29 (10) (1989) 809.
2. A.J. Moses, IEEE Proc. 137 (Part A5) (1990) 233.
3. K. Matsumura, B. Fukuda, IEEE Trans. Magn. MAG-20 (5) (1984) 1533.
4. J.T. Park, J.S Woo, K Chang, J.Magn. Magn. Matter. 182 (1998) 381.
5. B. Cornut, A. Kedous-Lebouc, Th. Waeckerlie, J. Magn Magn. Mater. 160 (1996) 102
6. Z. Akase, D. Shindo, Mater. Trans. 48 (2007) 10, 2626.
7. M. Li, Y. Xiao, W. Wang et al., Trans. Nonferrous Met. Soc. China 17 (2007) 74.
8. B.D. Cullity, Introduction to magnetic materials. Philadelphia, Addison Wesley Publishing Corp., 1972.
9. T. Nakayama and N. Honjou J. Magn. Magn. Matter. 213 (2000) 87.
10. O. Fischer, J. Schneider, Journal of Magnetism and Magnetic Materials 254 (2003) 302.
11. Steel statistical yearbook 2009, World Steel Association, World steel Committee on Economic Studies, Brussels, (2010) 55.
12. B. D. Cullity, C.D. Graham, Introduction to Magnetic Materials, 2nd Edition, John Wiley & Sons (2009) 439.
13. B. D. Cullity, C.D. Graham, Introduction to Magnetic Materials, 2nd Edition, John Wiley & Sons (2009) 455.
14. Yabumoto M. et al., Electrical Steel Sheet for Traction Motors of Hybrid/Electric Vehicles, Nippon Steel Technical Report No.88, (2003) 7, 57.
15. T. B. Massalski: Binary Alloy Phase Diagrams, ASM, Materials Park, Ohio, 1991, 1772

16. EN 10106:2009 – Cold rolled non-oriented electrical steel sheet and strip delivered in the fully processed state.
17. http://www.acroni.si
18. Hirsch J. and Lücke K., Acta Metall. 36 (1988) 2863.
19. Wenk H.-R., "Preferred Orientation in Deformed Metals and Rocks: An Introduction to Modern Texture Analysis", Academic Press, Orlando (1985).
20. Aernoudt E., Van Houtte P. , Leffers T., 'Deformation and textures of metals large strain', in "Materials Science and Technology", R.W. Cahn (ed.), 6 (1993) 89
21. Barrett C.S. and Massalski T.B., "Structure of Metals: Crystallographic Methods, Principles and Data", Pergamon Press, Oxford (1980).
22. V. Randle and O. Engler: Introduction to Texture Analysis: Macrotexture, microtexture and Orienattion Mapping, Gordon and Breach Science Publishers, 2000
23. Hirsch J. , Lücke K., Acta Metall. 36 (1988), 2863.
24. U.F. Kocks; Texture and Anisotropy: Preferred orientations in polycrystals and their effect on materials properties, Cambridge University Press, 1998.
25. Wenk H.-R., "Preferred Orientation in Deformed Metals and Rocks: An Introduction to Modern Texture Analysis", Academic Press, Orlando (1985).
26. Bunge H.J., "Texture Analysis in Materials Science – Mathematical Methods", Butterworths, London (1982).
27. J.A. Szpunar, in: H.J. Bunge (Ed.), Texture, Anisotropy in Magnetic Steels, Direction Properties of Materials, Cuvllier Verlag, Gttingen, (1988) 129.
28. Bessieres, J., Heizmann, J.J. and Eberhardt, A., Textures and Microstructures, (1991) 14, 157

29. Hatherly M. and Hutchinson B., "Introduction to Textures in Metals", vol. 5, Institution of Metallurgists, Chameleon Press (1979).
30. Bunge, H.-J. (Ed.), Theoretical Methods of Texture Analysis, DGM Informationsgesellschaft, Oberursel, Germany (1987)
31. Goto, T. Shimanaka, T. Irie, K. Matsumura, H. Nakamura and Y. Shono: in Proc. on Soft Magnetic Materials 3 (1977) 472.
32. H. Huneus, K. Günther, T. Kochmann, V. Plutniok, and A. Schoppa, "Nonoriented magnetic steel with improved texture and permeability," J. Mater. Eng. Perform., vol. 2, 199
33. A. De Paepe, K. Eloot, J. Dilewijns, and C. Standaert, "Effect of hot rolling parameters on the magnetic properties of a low-silicon ultralow- carbon steel," J. Magn.Magn. Mater., vol. 160, 129
34. H. Yasihiki and Okamoto, "Effect of hot band grain size on magnetic properties of non-oriented electrical steels," IEEE Trans. Magn., vol. 23, 3086.
35. M. Hatherley and W.B. Hutchinson; An introduction to textures in Metals, Chamelon Press Ltd., London, 1979.
36. H. Inagaki, "Effect of initial grain sizes on the development of rolling and recrystallization textures in polycrystalline iron," Z. Metallkd., vol. 82, 265.
37. Y. Hayakawa, J.A. Szpunar Acta matter. 45 (1997) 1285.
38. Y. Hayakawa and J.A. Szpunar Acta matter. 45 (1997) 4713
39. H. Shimanaka, Y. Ito, K. Matsumura, J. Magn. Magn. Mater. Vol. 26 (1982) 57
40. J.A. Szpunar, H.J. Bunge (Ed.), Texture, Anisotropy in Magnetic Steels, Directional Properties of Materials, Cuvllier Verlag, Gttingen, (1988) 129

41. F. J. Humphreys and M. Hatherly, Recrystallization and Related Annealing Phenomena, Pergamon Press (1995).

42. B. Cornut, A. Kedous-Lebouc, J. Magn. Magn. Mater. 160 (1996) 102.

43. R.E. Lenhart , J. Appl. Phys. (1964) 35**,** 861;

44. P. Van Houtte, Manual of MTM-FHM, MTM-KULeuven, Belgium, 1995

45. http://www.fei.com/products/scanning-electron-microscopes/quanta.aspx/

46. S.D. Likhithe, Prachi Likhithe and S.Radha ,AIP Conf. Proc. 1349, 49

47. T. Waeckerle, M. Mekhiche, C. Brun, J. Magn. Magn. Mater. 133 (1994) 195.

48. P.K. Rastogi, IEEE Trans. Magn. MAG-13, 5 (1977) 1448.

49. J. H. Scofield, Review of Scientific Instruments (1987) 58, 985.